

# High V

## Team 42 Project Technical Report to the 2018 Spaceport America Cup

Thomas Châteauvert<sup>1</sup>, Jonathan Bédard<sup>2</sup>, Alexandre Rivard<sup>3</sup>, Edouard Demers<sup>4</sup>, Maxime Guillemette<sup>5</sup>, Louis-Philippe Drolet<sup>6</sup>, Jean-Christophe Blais<sup>7</sup>  
*Laval University, Quebec, QC, G1V 0A6, Canada*

During the last year, GAUL has been working on its fifth high power rocket to compete in the 10,000 ft AGL apogee category. The design and manufacturing processes were documented and are presented in this report. The vehicle named High V is equipped with student-engineered parachutes, CO<sub>2</sub> deployment, Pitot tube, CubeSat with integrated acquisition systems, reinforced frame and a Bragg grating strain gauge. The payload is a fiber optic gyroscope which will be participating in the payload competition. Throughout the year, a lot of emphasis was put on integrating both electrical and mechanical components in a symbiotic manner. To do so, engineering leads put forward integration meetings in which students could exchange on how to incorporate their work to the design. This new initiative made the assembly of the rocket easier, but also demonstrated the strength of the GAUL as a multidisciplinary project.

### Nomenclature

C <sub>s(h)</sub>	= speed of sound as a function of the altitude [m/s]
P <sub>0</sub>	= atmospheric pressure at sea level [Pa]
P(h)	= atmospheric pressure as a function on the altitude [Pa]
G	= shear modulus of the material [Pa]
T = $\frac{t}{cr}$	= normalized thickness
B = $\frac{b^2}{s}$	= the aspect ratio of the fin
$\lambda_{\square} = \frac{c_{\square}}{cr}$	= fin taper ratio
C <sub>□</sub>	= root cord [m]
$\phi_s$	= phase shift [rad]
L	= length of the coil [m]
D	= diameter of the coil [m]
Λ	= wavelength of the laser [m]
c	= speed of the light
Ω	= angular speed [rad/s]
f <sub>m</sub>	= modulation frequency [Hz]
τ	= propagation time of the light in the coil [s]

<sup>1</sup> Structural team lead, Mechanical Engineering Department, thomas.chateauvert.1@ulaval.ca

<sup>2</sup> Structural team member, Mechanical Engineering Department, jonathan.bedard.8@ulaval.ca

<sup>3</sup> Structural team member, Mechanical Engineering Department, alexandre.rivard.7@ulaval.ca

<sup>4</sup> Structural team member, Mechanical Engineering Department, edouard.demers.1@ulaval.ca

<sup>5</sup> Avionics team lead, Electrical & Computer Engineering Department, maxime.guillemette.2@ulaval.ca

<sup>6</sup> Technical Director, Electrical & Computer Engineering Department, louis-philippe.drolet.1@ulaval.ca

<sup>7</sup> Director, Electrical & Computer Engineering Department, jean-christophe.blais.1@ulaval.ca

## I. Introduction

THE aerospace Group from Laval University (GAUL, acronym in French) is a student project from Laval University in Quebec, Canada. This team is composed from members of several science and engineering branches. The majority are from programs like Mechanical Engineering, Electrical and Computer Engineering and Physics Engineering while some are from programs like Chemical Engineering, Physics and Mathematics and Computer Science.

GAUL is divided into 5 teams. The first one is the direction team which is composed of the director, the technical director, the leader of each design and production team (Aerostructure, Avionic, Payload and Propulsion) and every other role that is important to the success of every aspect of the project (finance, website, sponsorship, recruitment, etc...). The others four teams are the Aerostructure, Avionic, Payload and Propulsion teams and are composed of their leader and members.

To achieve our final goal, each team meets once a week to work on different aspects of the project. Twice a month, the direction team meets to update everyone about the project progress and discuss the integration of the different parts. The following report will present the works done by the students on multiple new features on the rocket, like homemade parachutes, Pitot tube and a Bragg grating strain gauge and the improvement on the CO<sub>2</sub> deployment and the fiber optic gyroscope. First, we will present the system architecture overview and discuss about the propulsion, aerostructure, recovery, avionics and payload subsystems. We will then discuss about the Mission Concept of Operations (CONOPS). Finally, the lessons learned through the last year will be presented.

## II. System architecture overview

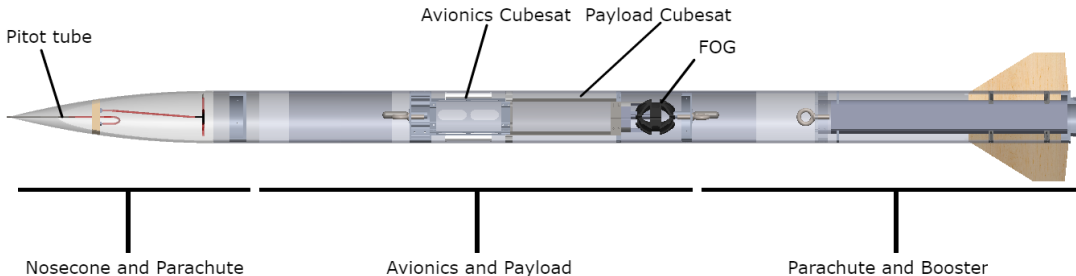


Figure 1. Overall view of the rocket

Our rocket, High V, is divided into three sections. As we can see on the figure 1, the booster section contains the motor, the Bragg grating drogue parachute. The middle section contains the avionics, the recovery system and the payload. There are also the CO<sub>2</sub> cartridges on each side of this section. Finally, we have the upper section which contains the main parachute and the nosecone.

### A. Propulsion Subsystems

For the propulsion subsystem, we are using a commercial off-the-shelf motor. To choose the motor we iterate over the possible engine by varying the mass of the rocket. We ended our choice with the CTI 9994-M3400-WT-P from Cesaroni Technology. Since in the last years we had problem with rocket that were too heavy for the chosen motor at the end of each build, we decided to buy the most powerful rocket in our size range manufactured by Cesaroni and we will add weight if we need to. The rocket is currently 72 lbs with a dead weight of 8.5 lbs for a predicted apogee altitude of 10039 feet. More detail can be found in the Appendix A.

### B. Aero-structures Subsystems

The following sections of the various Aero-structures subsystems thoroughly describes the design process, research and improvements done to the rocket and methods of fabrication. All the design process is first introduced, and the fabrication concludes this section. The pitot tube, a novelty in the 2017-2018 edition, is first described followed by its host, the nose cone. The structure receiving the avionics and the payload follows while the launcher section concludes the design section. After, the various fabrication methods are outlined.

### 1. Pitot Tube

The first subsystem is the Pitot tube. “The Pitot-static tube provides a simple, relatively inexpensive way to measure fluid speed. Its use depends on the ability to measure the static and stagnation pressures.”<sup>8</sup> “It is used in a wide range of flow measurement applications such as air speed in racing cars and Air Force fighter jets. In industrial applications, pitot tubes are used to measure air flow in pipes, ducts, and stacks but also with liquid flow in pipes, weirs, and open channels”<sup>9</sup>. Since it is such a common and widely used measurement, the 2017-2018 edition of the GAUL rocket added it.

The first couple of weeks of the Fall semester were spent researching different resources on Pitot tube designs and velocity equations. Fundamentally, the equation that yields the velocity, in an incompressible flow, is simply the difference between the static and dynamic pressures:

$$V = \sqrt{\frac{2\Delta p}{\rho}} \quad (1)$$

Where  $\Delta p = p_{static} - p_{dynamic}$ .

In fact, during the 10 000 feet target altitude flight of the GAUL rocket, there are two different flow regimes, subsonic incompressible and subsonic compressible. Inevitably, these two different regimes yield two distinct equations. The equation for the subsonic flow regime, i.e. Mach number below 0.3, is the Equation 1 above. For the latter regime, the equation is the following:

$$V = \sqrt{\frac{2\gamma p_{static}}{\gamma-1} \left( \frac{p_{stagnation}}{p_{static}} - \frac{(\gamma-1)}{\gamma} \right) - 1} \quad (2)$$

Considering the two equations, our Pitot tube needs to have sensors measuring the static and dynamic pressures, the air density and the altitude to read the heat capacity ratio ( $\gamma$ ). Since this equation requires the measurement of the air density during the flight, another avenue was considered.

Another approach to the velocity measurement equation can be realized with the Mach number. The static and dynamic pressures still have to be measured, but if the temperature at the stagnation point is known, the Mach number can be identified, and the velocity evaluated. The ambient temperature can be calculated with the stagnation temperature with the following equation:

$$T = T_0 \left( \frac{p}{p_0} \right)^{\frac{k-1}{k}} \quad (3)$$

With

$$1 + \frac{k-1}{2} Ma^2 = \frac{T_0}{T} \text{ so } Ma = \sqrt{\frac{2(\frac{T_0}{T}-1)}{k-1}} \quad (4)$$

And

$$c = \sqrt{kRT} \quad (5)$$

the equation for the rocket speed is

$$V = c * Ma \quad (6)$$

and after simplifications we obtain

$$V = \sqrt{\frac{2kR(T_0-T)}{k-1}} \quad (7)$$

Where k is the heat capacity ratio, R is the gas constant of air,  $T_0$  is the temperature measured at the stagnation point and T is the ambient temperature calculated with  $T_0$ .

This selected approach is better because the temperature at the stagnation point, the tip of the nose cone, is easier to measure than the air density.

---

<sup>8</sup> Munson, B.R., Okiishi, T.H., et al. *Fundamentals of Fluid Mechanics*, Wiley Editions, Seventh Edition, p.116

<sup>9</sup> <https://www.omega.co.uk/literature/transactions/volume4/pitot-tube.html>

Once again, the heat capacity ratio needs to be known. The selection of the velocity equation consequently affects the design of the Pitot tube. The latter approach with the Mach number was selected. At this point, we knew we needed to measure both the static and dynamics pressures, and the temperature. The heat capacity ratio varies only slightly with altitude and is then kept constant.

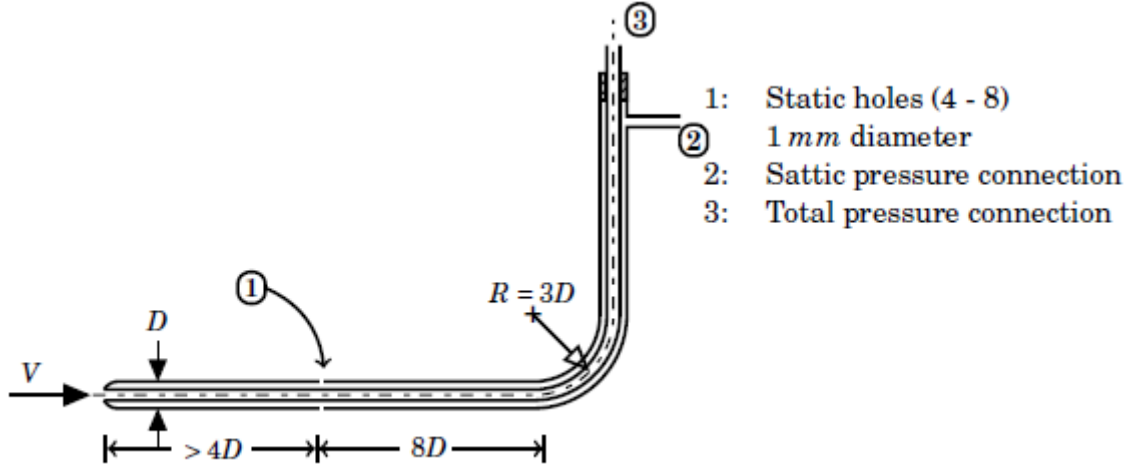


**Figure 2. Pitot static tube showing typical proportions**

In terms of design, our initial thoughts oriented towards a classic Pitot-static tube design which would stick out of the nose tip such as the one illustrated in the **Erreur ! Source du renvoi introuvable.**<sup>2</sup> above<sup>10</sup> (without the right angle).

Briefly, this design consists of measuring the dynamic pressure through a tube while the static pressure is measured with several holes along the tube. The dynamic and static flows then converge separately to be measured with different sensors. In order to have a precise measurement of both pressures, this design needs to respect certain principles. The geometry of the tip, the position of the static holes and the size of the holes all have an impact on the measurement. First of all, the tip of the tube affects the precision of the pressure measurement. The Figure 3Figure 3 below presents the impact of the angle of attack on the measurement<sup>11</sup>.

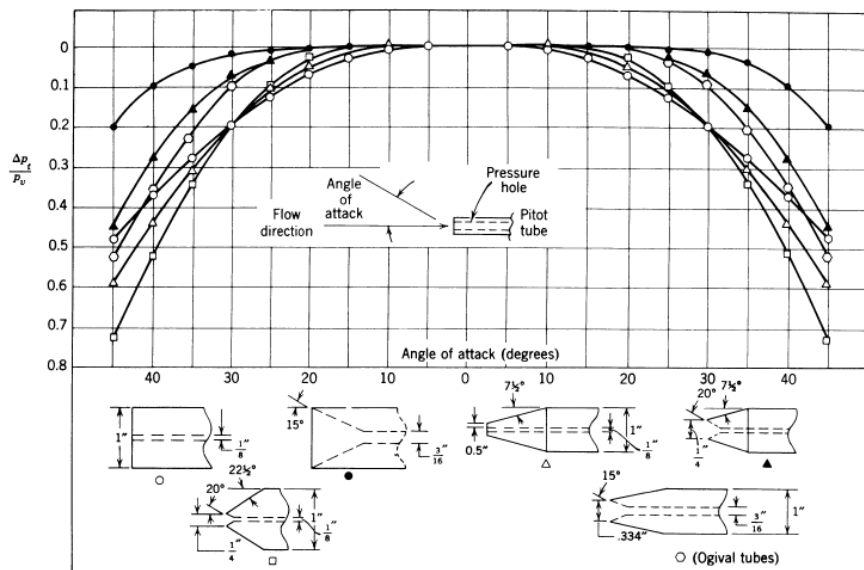


**Figure 3. Characteristics of several Pitot Tubes in regard to flow alignment**

<sup>10</sup> Venkateshan, S.P., *Mechanical Measurements*, Wiley Editions, Second Edition, p.284

<sup>11</sup> Benedict, R.P., *Fundamentals of Temperature, Pressure and Flow Measurements*, Wiley Editions, Third Edition, p.362

Next, the position of the static holes also influences the precision of the measurement. The Figure 4 below illustrates the impact of both the stem effects and the nose effects.<sup>12</sup> Since the tube is inserted in the nose cone and exceeds it, the selected design has a stem effect. Not only is the position of the static holes important, the size of the inner and outer diameters also is. The **Erreur ! Source du renvoi introuvable.** presented below enlightens the diameter selection.<sup>13</sup> The classic Pitot-static tube has a lot of peculiarities that need to be analyzed deeply before moving forward with a design. The impacts of the pressure measurement presented above has been discussed thoroughly throughout the semester and since they complicate greatly the design of the Pitot tube, we concluded that we needed another approach.

We then discussed our design issues with Professor Jean Lemay, who specializes in experimental measurements from our university, who directed us towards a more direct design consisting of stainless steel tubes, a thermocouple and pressure sensors. This design significantly reduces the imprecision in the measures while also being easier to integrate in the nose cone. The whole system is then integrated in the nose cone rather than having a bigger tube sticking out. The schematic presented in the Figure 4 below depicts our concept.

Starting from the top, there is a small stainless-steel tube,  $\frac{1}{8}$ " diameter<sup>14</sup> (1) that receives the flow destined to the dynamic pressure. The small tube minimizes the effect of having a hole directly at the tip of the nose cone (7), i.e., the bigger the hole, the greater the drag. Next to this tube, is a thermocouple to measure the stagnation temperature<sup>15</sup>. Considering the fact that the rocket flies rapidly, the altitude consequently increases swiftly. In order to measure the temperature precisely, a very thin thermocouple, type K, with a short time constant is selected. This small tube is welded to a bigger stainless-steel tube (2),  $\frac{3}{16}$ " diameter<sup>16</sup>. Finally, a vinyl tube (3) connects the stainless-steel tube (2) to a dynamic pressure sensor (5)<sup>17</sup>.

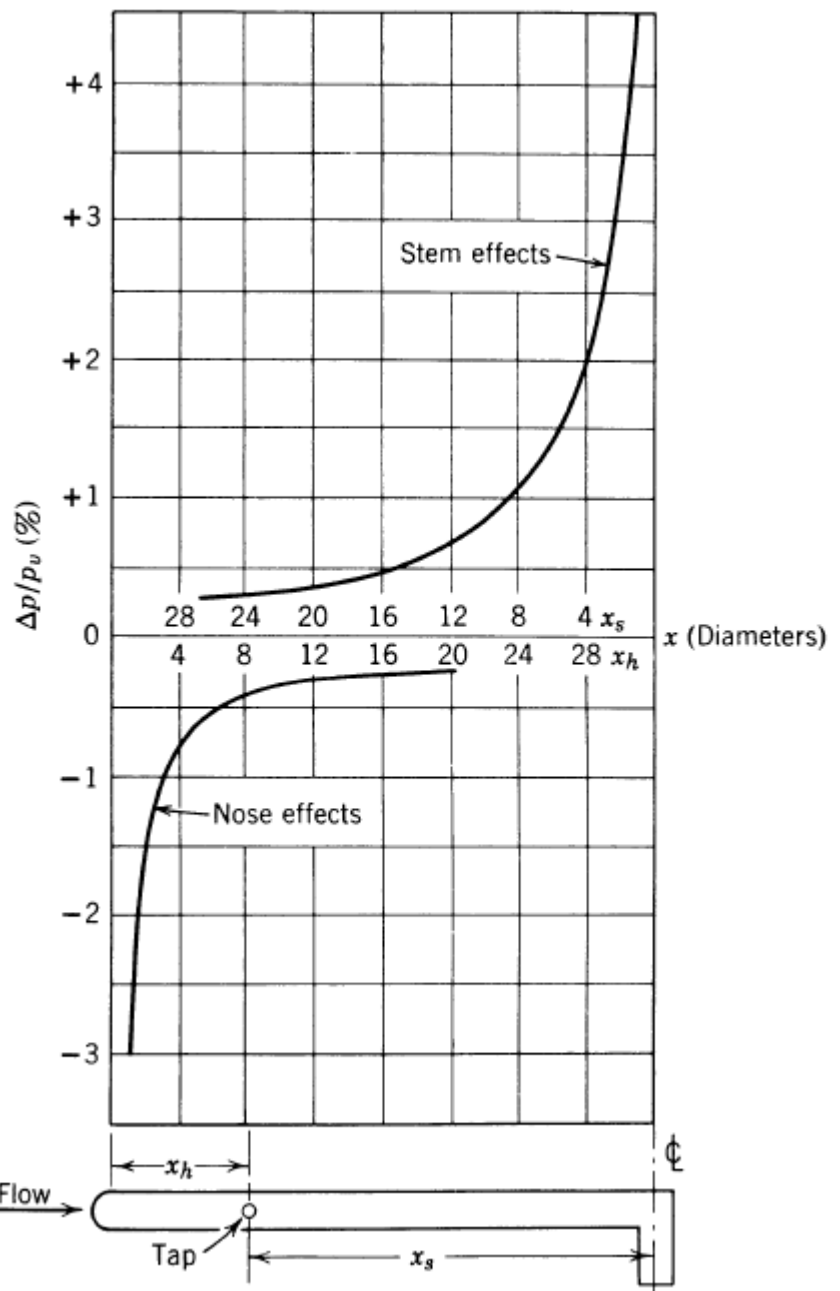


**Figure 4. Effect measure in percentage vs the inner and outer diameter**

The graph plots the effect measure in percentage ( $\Delta P/P_v \%$ ) against the inner and outer diameter ratio ( $x$ ). The top curve, labeled 'Nose effects', shows a rapid increase from approximately -3% at  $x=4$  to about +4% at  $x=28$ . The bottom curve, labeled 'Stem effects', shows a much slower increase, starting near 0% at  $x=4$  and reaching about +1% at  $x=28$ .

<sup>12</sup> Ibid.

<sup>13</sup> Russo, G.P. *Aerodynamic Measurements*, Woodhead Publishing, First Edition, p.31

<sup>14</sup> <https://www.mcmaster.com/#catalog/124/170/=1cuwzkj>

<sup>15</sup> [https://www.omega.ca/pptst\\_eng/irco\\_chal\\_p13r\\_p10r.html](https://www.omega.ca/pptst_eng/irco_chal_p13r_p10r.html)

<sup>16</sup> <https://www.mcmaster.com/#catalog/124/170/=1cux0ks>

<sup>17</sup> <https://www.digikey.ca/products/en?keywords=MPXHZ6250AC6T1CT-ND>

At the other end, four small holes are drilled in the nose cone to collect stagnant air for the static pressure. These holes need to be the furthest from the tip or any curvatures in the nose cone in order to obtain a precise measure. Curves around a body accelerate the flow which induces a misreading in the static pressure measurement. Once again, short stainless-steel tubes (2) collect the air through these holes. Vinyl tubes (3) connect the stainless-steel tubes to a 3D printed homemade fitting (6) as seen in the Figure XX below. This fitting has four inputs and one output. Finally, another vinyl tube connects the output of the fitting to the static pressure sensor<sup>18</sup> (4). Both sensors are connected on a printed circuit board PCB (8). Many other components on the PCB are not shown purposely (capacitors, resistances, batteries, etc.). The pitot tube PCB is further explained below.

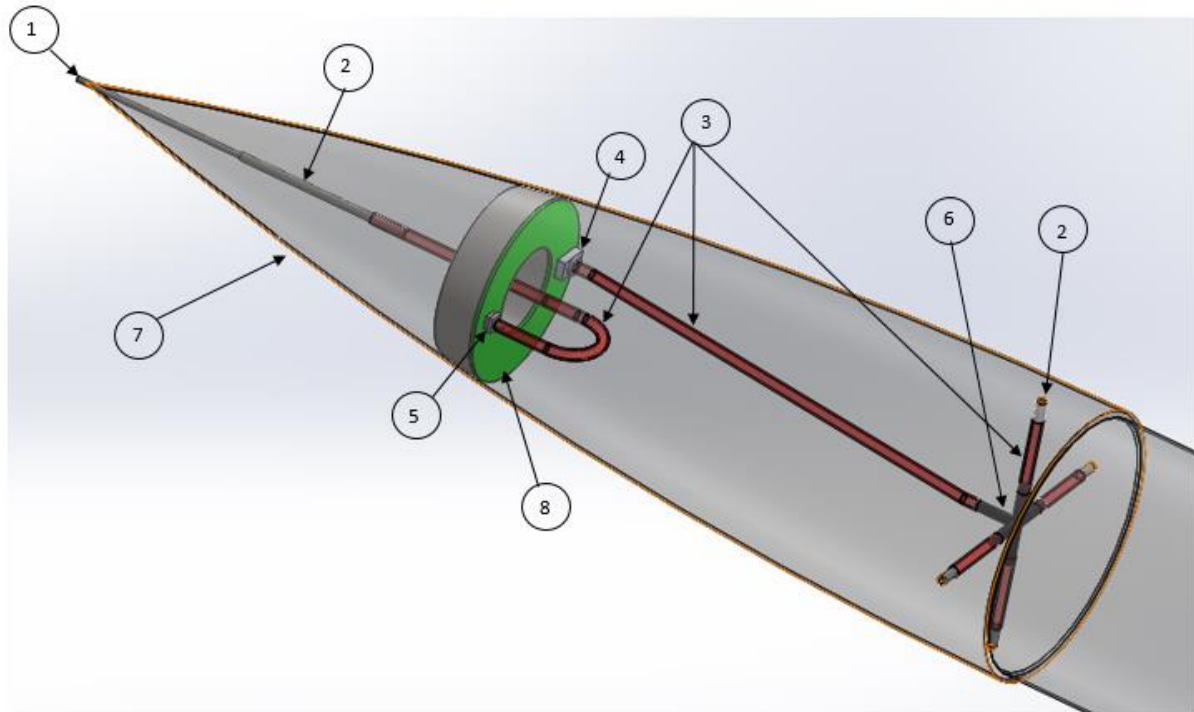


**Figure 5. Schematic of the Pitot tube installation**

This design significantly reduces the risks of a misreading in pressure measurement. The dynamic pressure sensor directly reads the pressure from the incoming flow. Following Prof. Jean Lemay's recommendations, four holes collect the stagnant flow in order to obtain an average static pressure measurement, again, to decrease the risk of imprecision. We have design a small piece that join the four holes, like shown in the **Erreur ! Source du renvoi introuvable**.<sup>6</sup> Those imprecisions may occur from the changing orientation of the rocket that alters the pressure difference on both sides of the nose cone or the unbalanced mix of the four static pressure intakes.

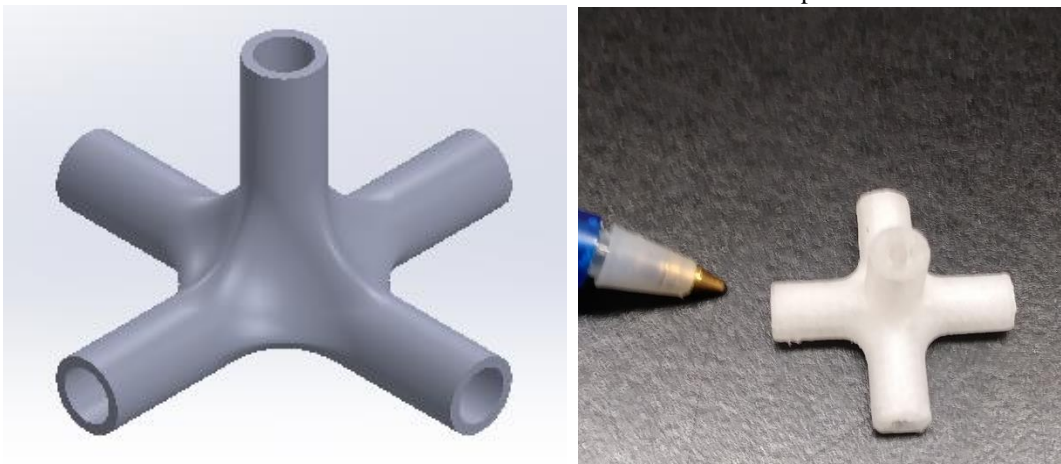


**Figure 6. Schematic and 3D printed part for the static coupler**

<sup>18</sup> <https://www.digikey.ca/products/en?keywords=MPXHZ6115AC6U-ND>

Our design and assembly completed, tests can be done on a protoboard to verify the robustness of the different connections (fitting fit between vinyl and stainless-steel tubes, connection with the pressure sensors, etc.) and the quality of the Arduino code. Since the GAUL has already built rockets in the past, it uses old nose cones as prototypes for the new design.

## 2. Nose cone

The last couple of rockets built by the GAUL inspire the 2017-2018 edition to stay conservative in terms of design, and to optimize different sections and components. Since the competition allows points for homemade components, this year's team decided to try to fabricate its own nose cone. We first met people from HTM Composites, specialized in the making of complex fiber, carbon or kevlar parts with the infusion process<sup>19</sup>, to discuss the possibility of fabricating our nose cone with fiberglass. They suggested to create a medium density fiberboard (MDF) mold where they could add the fiberglass inside. They suggested to create a medium density fiberboard (MDF) mold where they could add the fiberglass inside. Unfortunately, the forestry department laboratory with the 5-axis computer numerical control (CNC) machine was not available for the project. We then tried to fabricate the nose cone ourselves.

Inspired by numerous YouTube videos, the Aerostructure team tried to create a polyurethane two-part mold. For the bottom part, clay served as the top half for reference while also playing a role in the demolding. Once the clay completely recovered one half, polyurethane was blown on the surface. The following figures illustrate the

The result of the first half was promising, the clay did a perfect job of separating the polyurethane mold in half. A myriad of glass balls made it easier to remove the polyurethane from the clay. Although both members on the picture above look satisfied, they didn't know what the result



**Figure 7. Nosecone mold picture 1**

of the second half would be. The first half completed, clay was removed, and polyurethane was once again blown to complete the mold. A sheet of polyethylene separated both halves of polyurethane.

Once the urethane had dried, the separation of both halves resulted in the destruction of the second half. The urethane did not completely dry in certain regions which made these areas very sticky and the demolding almost impossible. After several hours of research and work in the lab, only one half could have been used and therefore the nose cone had to be bought.



**Figure 8. Nosecone mold picture 2**



**Figure 9. Nosecone mold picture 3**

<sup>19</sup> [http://htmcomposites.com/index\\_en.html](http://htmcomposites.com/index_en.html)

Similar to the previous years, the GAUL relies on the FNC-6.0 fiberglass nose cone from Public Missiles<sup>20</sup>. The fiberglass can sustain the various stresses during the entire flight with acceleration reaching close to 12G. The empty nose cone makes it easier to introduce the Pitot tube, drill holes and install a structure to host the PCB.



**Figure 10. Nosecone mold picture 4**

### 3. *Homemade Retainer*

The Aerostructure division really emphasized on having a maximum of homemade components for this year's rocket. Following this idea, we completely redesigned the motor retainer, historically bought. We usually bought a retainer similar to the one illustrated on the right<sup>21</sup>.

Using such a retainer requires having another component fixed in the bottom section of the rocket in order to screw the retainer. The 2017-2018 design eliminates that extra component by combining these two components. Instead of having three parts, one fixed in the rocket, another one screwed and the cap, we now have one component fixed to the rocket and the cap. The new design is pictured below.



**Figure 11. Commercial motor retainer**

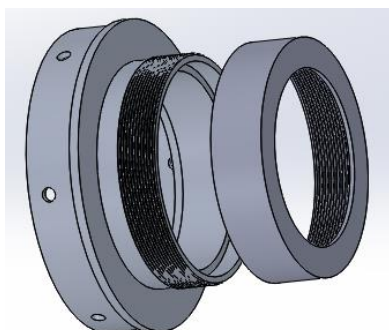


**Figure 12. Student designed motor retainer**

The retainer still has the function, i.e. to retain the motor in position but is now lighter and simpler to install. Unfortunately, the mechanical engineering machine shop at Laval University doesn't have 7-inch aluminum rod in stock and since the CAD was completed late in the Spring semester, the fabrication of a homemade retainer was not done. The motor retainer is recuperated from last year's rocket and use for this year's competition. Nevertheless, since the GAUL now has an improved and functioning new design for the motor retainer, next year's team will be able to use the drawings from the 2017-2018 edition.

<sup>20</sup> <https://publicmissiles.com/product/nosecones>

<sup>21</sup> [https://www.apogeerockets.com/Building\\_Supplies/Motor\\_Retainers\\_Hooks](https://www.apogeerockets.com/Building_Supplies/Motor_Retainers_Hooks)

#### 4. Avionics Bay

It is the third year that we use a 6-inch diameter rocket design, the first one was Ragnarok, then Menhir. Like last year, we've made improvements on the assembly of the avionics bay, learning each times from the design flaws of the previous years. The main flaw with Project Menhir's avionics, was the amount of screws that needed to be perfectly aligned between the bulkheads and the fuselage. Since every holes were drilled by hand, it needed a specific angle and a specific height of the bulkhead in order to be able to secure the avionics. Below you can see Menhir's avionic assembly, then our current design.

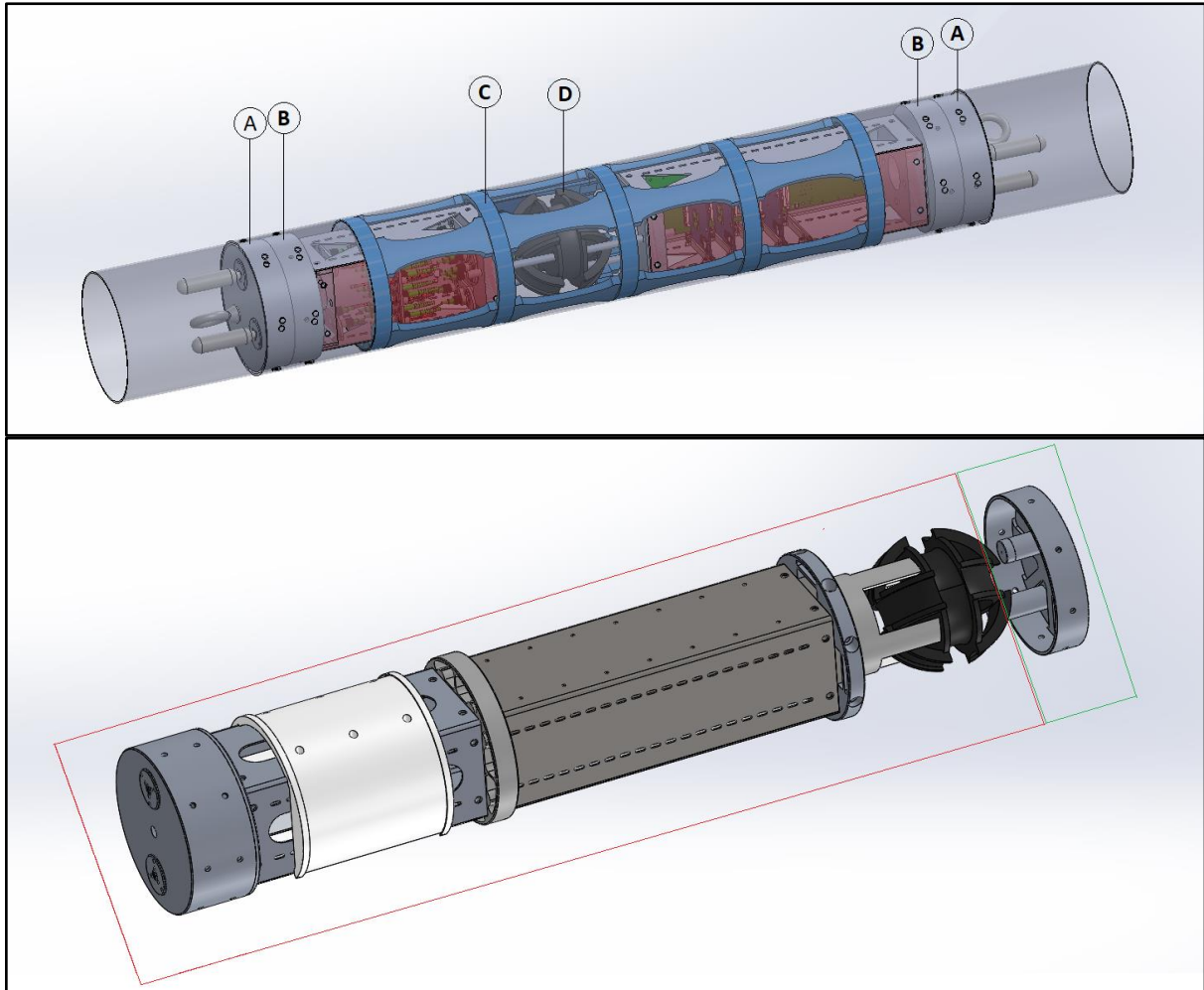


**Figure 13. Comparison of Menhir and High V avionics and payload bay**

The assembly shown in the first picture required a rail guide (C) for the cubesat. There were 5 assemblies that needed to be stacked, aligned and screwed to each other: two bulkheads (A), two retainers (B) and the cubesat assembly - gyroscope (D). This design also required to have loose cables on both sides to connect the deployment, which made it harder to assemble. The avionic had too much space in the 3U cubesat and the payload had too little in the 2U.

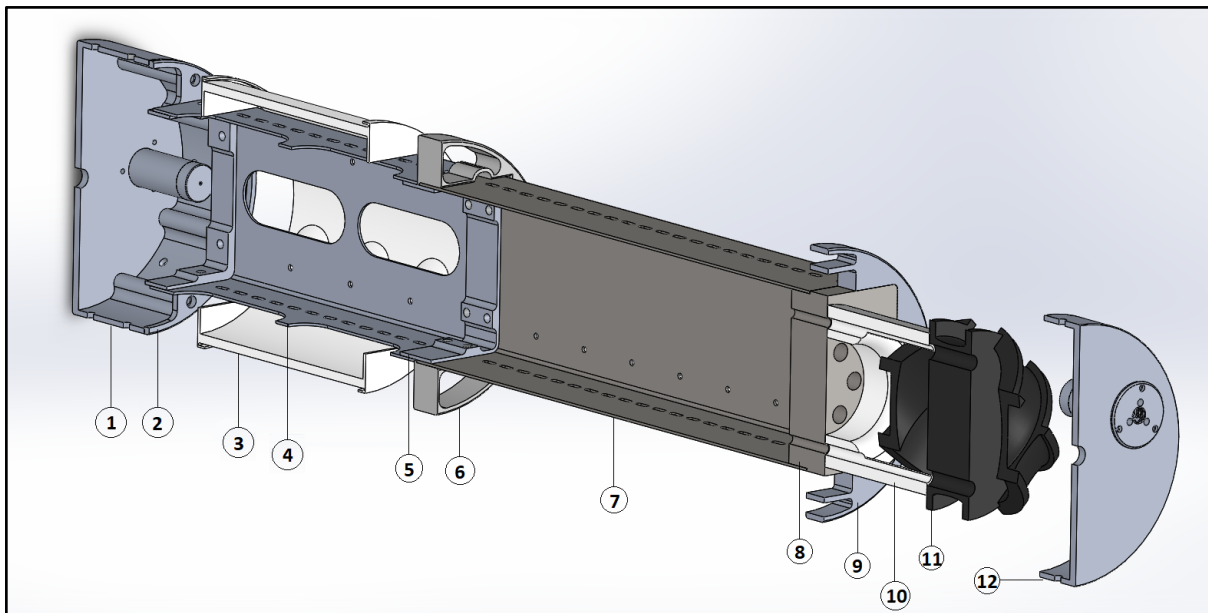


**Figure 14. High V avionics and payload bay assembly**

In this year's design, there are only two assembly: the upward bulkhead (1) - cubesats (4-7) - gyroscope (11) and the downward bulkhead (12). Here the gyro is closer to the center of mass of the rocket, making its readings more accurate. Another important improvement is that the whole structure will slide in the fuselage without the need of rails. The disc (9) serve as a centering ring and a shoulder which will sit on the bottom coupler so that during the launch, it is the coupler that takes most of the weight of the avionic and when the main parachute deploys, the set of screws on the upper bulkhead (1) take the choc of the fuselage and the booster stage, but not the avionic. Because the bulkhead (1) is part of the assembly and slides with it, there is no need to have loose cables on this side and there is plenty of space around the gyro to push the excess cables.

The actual avionic is located in the 2U cubesat (4) and the 3U (7) is for the payload. We slightly modified the design for the cubesats. Because they are stacked next to each other, there is no need to close the connecting sides, therefore using less metal and being lighter. Many components were optimized to reduce the weight besides the required 4kg of the payload. That is why the component (8) is a big chunk of steel. The middle centering ring (6) is 3D printed in PLA because its only purpose is to help the sliding process. The component (3) is also 3D printed and is meant to slide on its contour an insect-fed patch antenna. The component (10) is a 3D printed object on which sits the gyroscope (11) at the right height and helps to protect and to contain the optic fibers.

##### 5. Fuselage fabrication

Since a couple of years, the GAUL buys phenolic tubes for the fuselage of its rockets and enforces it with carbon fiber for one section and glass fiber for another. At the beginning of the fall semester, the goal of the Aerostructure division was to modify the fabrication process by exploring new avenues such as filament winding or water-soluble materials. Since a few of the members have 3D printers, tests on a water-soluble 3D printing material, polyvinyl alcohol (PVA), were conducted. The goal of the test was to compare the strength of the tube with the phenolic tubes the Club usually buys.

Solid polylactic acid (PLA) tubes were first printed. These were meant to ensure a circular shape since we planned to use a minimal amount of PVA because the material is expansive. The PVA tubes were printed at two shells thick (the walls of the tubes had a thickness of 0.8 mm). Layers of carbon fiber were then directly applied on the PVA and then put in a water bath for 24 hours. Therefore, the PVA dissolves and we are left with a carbon fiber tube. Figure 15 below shows the tube in the water solution and the final carbon fiber tube, with the PVA dissolved, is pictured on Figure 16.



**Figure 16. Carbon fiber test tube in water**

obtain a 7 feet high fuselage.

To solve the second problem, a different PLA core tube that facilitates the water flow through the PVA was designed and made, but due to the quality of the PVA used and the random cases of print failure, we decided this process was not a viable option.

Even though it was a great learning experience using relatively new technologies such as 3D printers and water soluble printed materials, the old fabrication processes were much easier and faster.

On the other hand, a couple members of the Aerostructure division read and learned about filament winding. Figure XX<sup>22</sup> lays out an example.



**Figure 15. Carbon fiber tube without the PVA**

Although a clean carbon fiber results of this test, this process had many challenges to overcome. First, the PVA tube was hard to print because the material is very brittle and the 3D printer's nozzle clogs easily. Second, the PVA never dissolved completely because the water had only 0.8 mm to flow between the PLA and the carbon fiber. The PLA had to be broken down with a hammer in order to extract the carbon fiber tube. Finally, since 3D printers have limited dimensions to print, numerous sections would have to be assembled together in order to

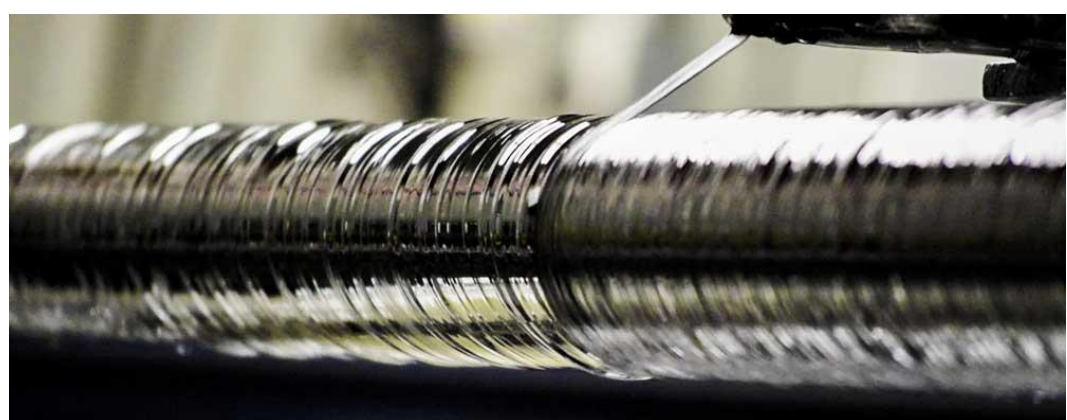


**Figure 17. Filament winding**

<sup>22</sup> <https://woundupcomposites.com/filament-winding/>

This fabrication process has a significantly better surface finish than the wet layup process currently used by the GAUL and described in the following paragraph. Thus, switching processes would be a great advantage for the quality of our fuselage. After trying to contact several filament winding companies, a decision to create a winding machine was taken. The Aerostructure division soon realized all the various complexities of such a project. The synchronisation between the rotating speed of the tube and the linear velocity of the filament has to be perfect in order to attain a successful result. The machine also has to minimize the various disturbances such as the vibrations created by one or two electric motors. The carbon fiber filament has to be in contact with epoxy in order to stick to the fuselage tube. Although a couple of drawings were made as first drafts and discussions emerged, due to a lack of time, the filament machine was not designed. The information gathered this year will definitely serve as a great beginning for next year's competition.

So, after trying other venues, the Aerostructure division finally settled on the wet layup process. Let's begin with the bottom section, covered with carbon fiber. The 6 inch diameter Blue tubes are bought from Apogee Rockets<sup>23</sup>. They have high impact resistance and are also able to resist Mach number speeds. They are then covered with carbon fiber sheets, a sponsorship from Textreme<sup>24</sup>. In a nutshell, the wet layup process consists of applying the carbon fiber sheet directly on the tube and adding epoxy. 105 epoxy Resin<sup>25</sup> and 205 Fast Hardener<sup>26</sup>, both from West System are utilized for the mixture. Figure 18 below illustrates this process.



**Figure 18. The team working on the wet layup process**

Once 6 layers of carbon fiber are applied, the epoxy surplus is vacuumed through a vacuum bag. A pump runs for 12 hours to vacuum all the air that could have been introduced in between the layers. The following Figure 19 and 20 exhibit the vacuum bag process and the final result.



**Figure 19. Vacuum bag process**



**Figure 20. Final result for the wet layup for the structure**

<sup>23</sup>

[https://www.apogeerockets.com/Building\\_Supplies/Body\\_Tubes/Blue\\_Tubes/6in\\_Blue\\_Tube?zenid=h7vokncik2tk77e10kcong9ao5](https://www.apogeerockets.com/Building_Supplies/Body_Tubes/Blue_Tubes/6in_Blue_Tube?zenid=h7vokncik2tk77e10kcong9ao5)

<sup>24</sup> <http://www.textreme.com/>

<sup>25</sup> <https://www.westsystem.com/105-epoxy-resin/>

<sup>26</sup> <https://www.westsystem.com/205-fast-hardener/>

The bottom section of the rocket is covered with carbon fiber while the middle one is covered with glass fiber. The middle section has to be covered with glass fiber in order to be radio permeable since avionics components communicate with the ground station. This middle section is also made with the wet layup process.

Another goal set by the 2017-2018 GAUL program was to fabricate our own couplers. We found a new partner, HTM Composites<sup>27</sup>, who are specialized in a myriad of fiberglass processes. Through various discussions with one of the engineers, we settled on having them add fiberglass to phenolic couplers. That way, the couplers have a greater strength and can support greater stresses. The result is shown on Figure 21.



**Figure 21.** Student made coupler

#### 6. Carbon fiber fins

The fins of the rocket are made of  $\frac{1}{4}$ " plywood recovered with 3 layers of carbon fiber. The shape of the fins is further discussed in section B-7.

The process for applying the carbon fiber is the same as the fuselage, wet layup. In order to obtain a perfectly straight surface during the vacuum, a glass window is used and delineated in the following Figure 22 while Figure YY portrays the final result.

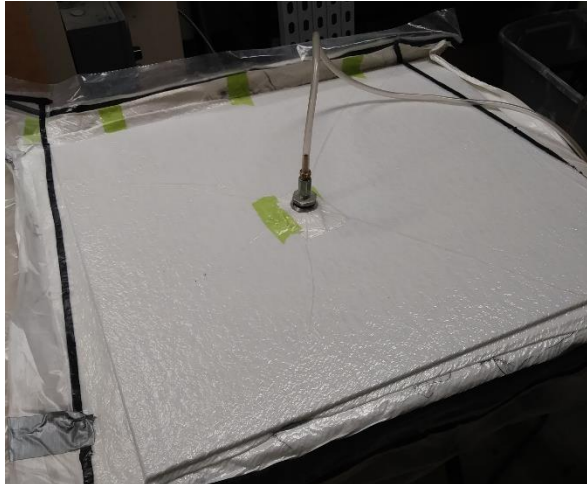


**Figure 23.** Wet layup with a glass window



**Figure 22.** Final result of the wet layup for the fins

#### 7. Fin Design

When designing fins, one has to be aware of the aerodynamic effects of slight modifications on the geometry. All other things being equal, the geometry of the fins directly impacts the altitude and the stability of the impact. For instance, increasing the length of the leading edge raises the altitude but also reduces the stability. The stability criteria is to have at least 2 calibers, i.e. two fuselage diameter lengths between the center of gravity and the center of pressure. Since the GAUL doesn't have expertise in fin design or Computational Fluid Dynamics (CFD) simulations, the result of Open Rocket<sup>28</sup> simulations dictate the design of the fins. In other words, once the fuselage length and weight estimate are known, several fin geometries are tested in OpenRocket. The goal of these various iterations is to obtain a compromise between stability and aerodynamics (target altitude). The following Figure 24 presents the final geometry (the dimensions are in millimeters).

<sup>27</sup> <http://htmcomposites.com/>

<sup>28</sup> <http://openrocket.info/>

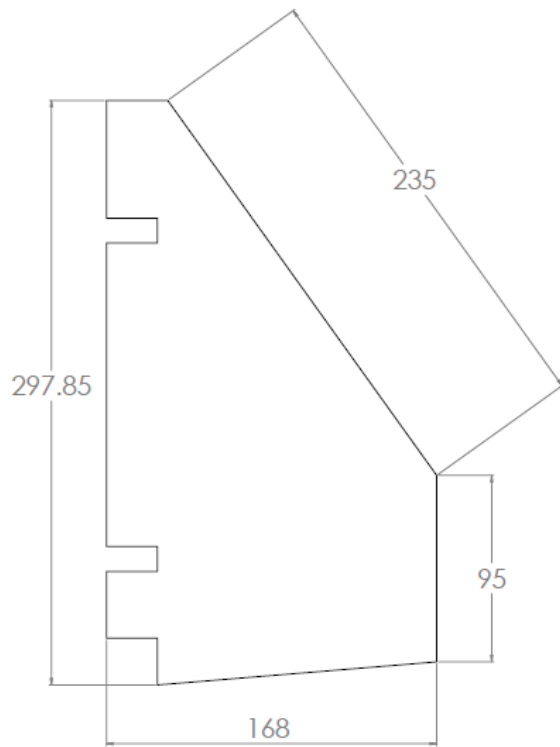


**Figure 24. Final fins geometry**

#### 8. Fin Flutter Analysis

The fin design goes hand in hand with the fin flutter analysis. Essentially, “flutter is an aeroelastic instability commonly seen in wings, tails, rotor blades and control surfaces of aircraft, as well as rocket fins. The phenomenon occurs when aerodynamic loads cause deformation of the body, which in turn creates a reaction by the structure, initiating an oscillatory motion”. <sup>29</sup> An example of the deformation of the fins on a rocket is illustrated below<sup>30</sup>.



**Figure 25. Fins flutter phenomena**

<sup>29</sup> <http://digitalcommons.calpoly.edu/cgi/viewcontent.cgi?article=1113&context=aerosp>

<sup>30</sup> [https://www.youtube.com/watch?v=pyct1Pii\\_cg](https://www.youtube.com/watch?v=pyct1Pii_cg)

Obviously, this phenomenon is to be avoided at all cost during the entire flight of the rocket. The flutter speed can be evaluated based on the geometry of the fins and compared to the velocity values of Open Rocket to confirm that the flutter phenomenon is not attained. The flutter speed is solved following the methodology elaborated in the Apogee Rocket Newsletter 411.<sup>31</sup> Based on a previous Newsletter<sup>32</sup>, the new issue simplifies the flutter speed equation, i.e.:

$$V_f = 1.223 C_s \sqrt{\frac{G}{P}} \sqrt{\left(\frac{T}{B}\right)^3 \left(\frac{2+B}{1+\lambda}\right)} \quad (8)$$

The flutter speed  $V_f$  depend therefore on the speed of sound  $C_s$ , as a function of the altitude,  $G$ , the shear modulus,  $P$ , the pressure, also as a function of altitude,  $T$  the normalized thickness, the ratio of the fin thickness over the tip chord,  $B$ , the aspect ratio, the fin height squared over the area and finally lambda, fin taper ratio, tip chord divided by the root chord. The newest Newsletter proposes a simplified formula based on atmospheric values. The final equation is:

$$V_f = 1.223 C_{s0} \exp(0.4 \frac{h}{H}) \sqrt{\frac{G}{P_0}} \sqrt{\left(\frac{2+B}{1+\lambda}\right)} \left(\frac{T}{B}\right)^{3/2} \quad (9)$$

The formula solely depends on the altitude  $h$  as the speed of sound and the pressure have been normalized to atmospheric values, 335m/s for the speed of sound  $C_{s0}$  and 101.3 kPa for the pressure. This equation is then used to evaluate the flutter speed based on our fin geometry. The result is illustrated below.

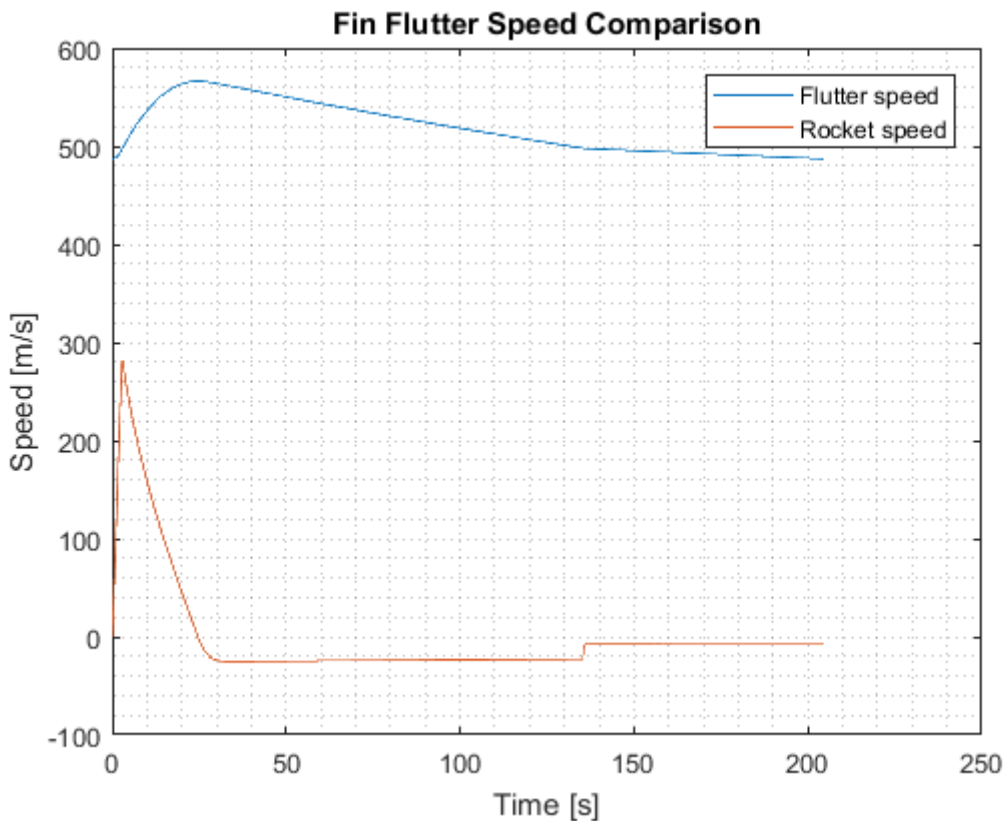


Figure 26. Fin flutter speed graphic

The flutter phenomenon, based on the calculation above, will not be observed since during the entire period of the flight, the flutter speed is above the rocket speed.

#### 9. Assembly of the bottom section

The assembly of the launcher section requires careful attention especially in the position and the alignment of the fins. In order to obtain a precise alignment, a 3D printed guide was used. It is made of several components due to the dimension limitations of the 3D printer utilized and since some parts are permanent to the rocket assembly while others are removed. Applying epoxy at the interface fins-motor tube was then much simpler while guaranteeing the angle of 120° between the three fins. The result is shown in the next page.

<sup>31</sup> <https://www.apogeerockets.com/education/downloads/Newsletter411.pdf>

<sup>32</sup> <https://www.apogeerockets.com/education/downloads/Newsletter291.pdf>

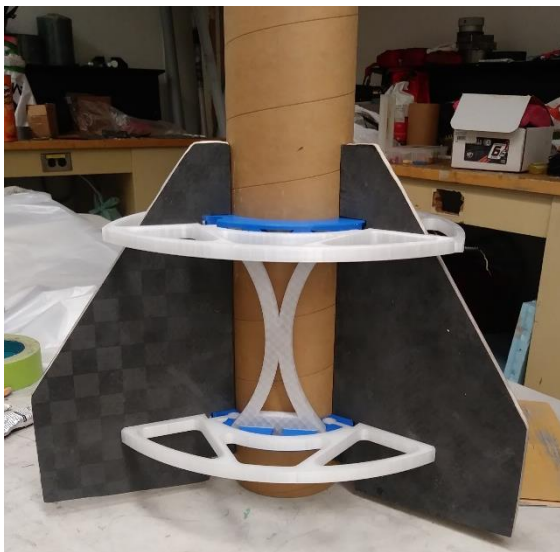


Figure 29 3D printed guide close up view



Figure 27. 3D printed guide top view



Figure 28. 3D printed guide overall view

Several fin guides have been used historically by the GAUL, but this year's version is unique since the centering rings of the guide will stay on the motor tube. So, there are removable parts in the guide (white material in the figures above) and permanent material (blue material in the figures). By doing so, the centering rings will be correctly placed in the bottom fuselage tube while being fixed to the fins. This simplifies significantly the assembly of the bottom fuselage section and guarantees a perfect alignment of the fins.

#### *10. Camera shroud*

Since last year, the GAUL introduced cameras in the rocket to have footage of the flight on two different angles, vertically and horizontally. An example of the footage obtained of the vertical view is shown below from a low altitude flight in Saint-Pie-de-Guire, Quebec.



**Figure 30. Footage from vertical camera**

A lot of the design process was done last year by elaborating the first camera shroud in the history of the GAUL. Last year's shroud is illustrated below.

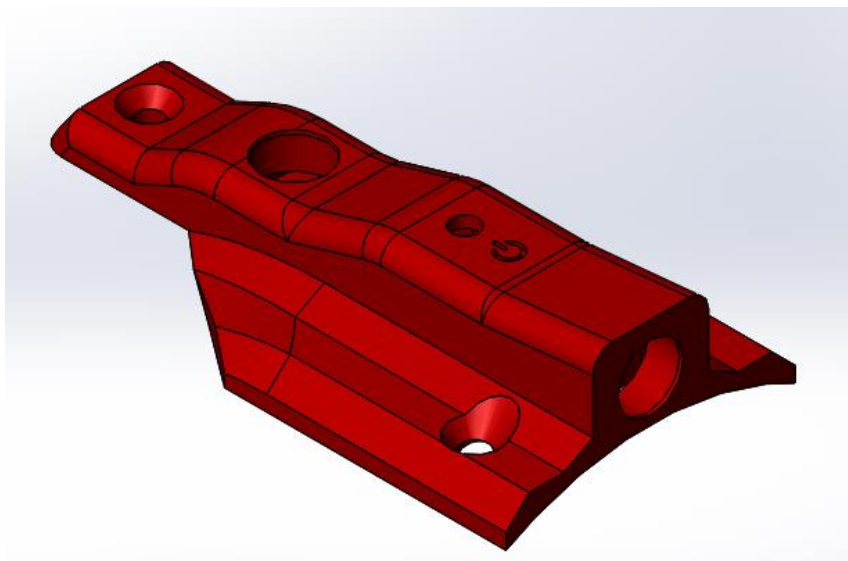


**Figure 31. Camera shroud CAD model**

Slight modifications have been made to this year's edition. The connections between the cameras and their electronic components were hard to realize during the assembly. Now, the batteries and the electronics are in the shroud instead of being fixed to the rocket. This year's design solves these various issues making the assembly easier. The design is yet to be finished so we don't have a final CAD version.

## C. Recovery Subsystems

### 1. CO<sub>2</sub> Deployment

To deploy the parachutes, we are using our own CO<sub>2</sub> system which has been in development for 3 years and this summer might be the perfect version of it. The previous version had three main flaws: instability of the striker due to the use of an O-ring, explosion of the bottom side where a 3D printed component houses the e-match and a not long enough threaded hole for the cartridge which caused the cartridge to get punched like a rivet.



**Figure 32. CO<sub>2</sub> deployment housing**

The current version (MK3) answers all those problems. First, instead of using an O-ring, we use a slide-fit plain bearing made of acetal plastic. That way, the striker can't change its angle and get stuck. Second, to prevent the plastic e-match holder from breaking, instead of screwing it from the outside, we now slide it from the inside and an aluminum wall absorbs the blast. Lastly, the threaded hole is slightly deeper according to the cartridge we use.

The Figure 33 below shows how it works.

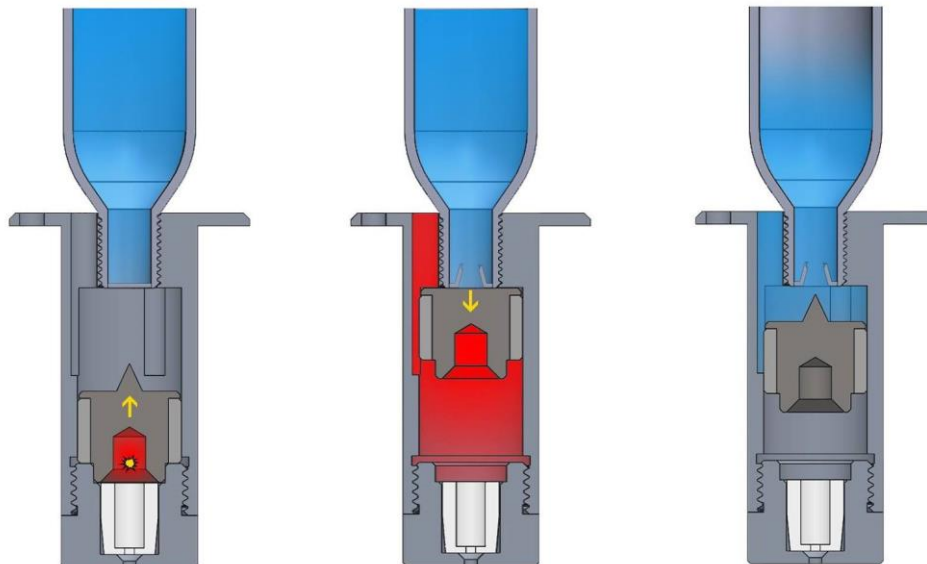


**Figure 33. CO<sub>2</sub> deployment mechanism**

We believe that our design is unique because both the blast of the black powder and the CO<sub>2</sub> escape from the same side using the same exhaust way. Furthermore, the electric cables are already inside the bulkhead while a Rouse Tech CD3 or a Peregrine design gets the cables on the same side as the exhausts. The use of an easily removable and disposable e-match holder makes it fairly easy to use and clean. The e-match is epoxied inside the plastic holder. A small dot of cyanoacrylate glue ensures that the striker stay in place during the launch. The only possible flaw comes from the slide fit tolerance. If we neglect the cleaning of the components after each use, the striker will no longer be able to move.

## 2. Fabrication of the parachutes

The idea of fabricating our own parachutes had been discussed for several years but no one really invested time in effort to actually fabricate them. This year, we started by fabricating two parachutes and compare the results. Since we didn't find any literature or design patterns for parachutes, the first iteration was solely based on previous bought parachutes. The first homemade parachutes are illustrated below.



**Figure 34. First iterations of the homemade parachutes**

The hardest part of making our parachutes is to find an efficient way to test them. We tried several options, dropping lightweights from several stories high, from the football stadium or an observation tower. The following snapshots illustrate these various tests.



**Figure 35. Homemade parachute droptest**

Although no data was required using an altimeter and or a gyroscope, the tests gave a lot of qualitative information as we tested the homemade parachutes and compared with a bought one from last year. Referring to the picture below<sup>33</sup>, some parachutes had a spill hole too small thus reducing considerably the drag while others had a canopy-diameter ratio too big also reducing the drag.

With all that information, we had all the tools to design the main and the drogue parachutes for the competition rocket.

### *3. Design of the parachute*

The key word for making these parachutes was “toroidal”. A torus is a surface of revolution generated by a circle revolving around a certain axis. Because it is mathematically proven that a flat surface (i.e. the parachute fabric) cannot be transformed into a toroidal shape without being stretched, thus applying unnecessary stress on the fabric, the parachutes are made out of a series of panels to minimize this effect.

We had to generate equations to determine the width and length of each panels.

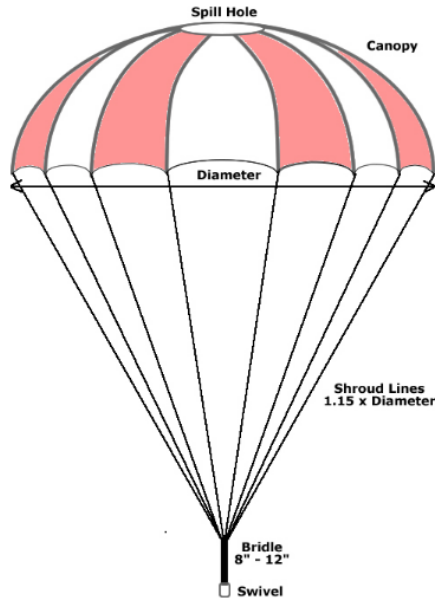


**Figure 36. Parachute design**

---

<sup>33</sup> [https://fruitychutes.com/help\\_for\\_parachutes/how\\_to\\_make\\_a\\_parachute.htm](https://fruitychutes.com/help_for_parachutes/how_to_make_a_parachute.htm)

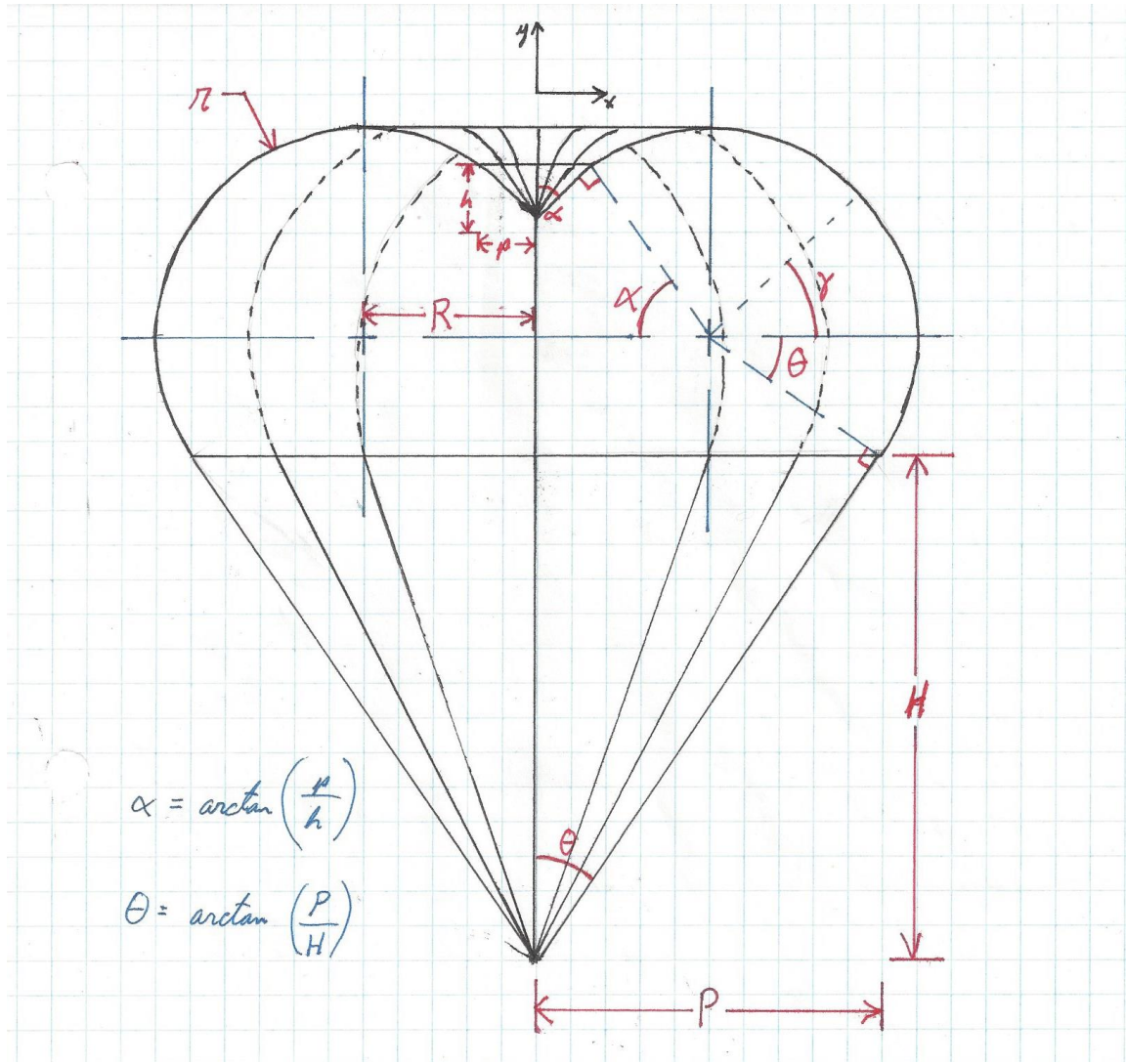


**Figure 37. Parachute schematic**

Based on this cross-section view of the parachute, the length of a panel is equal to the length of the circle arc defined by the equation  $L = r(\theta + \pi - \alpha)$ , where  $r$  is the radius of the revolving circle,  $\theta$  is the angle between the horizontal plane and the exterior border of the parachute measured from the exterior of the parachute in radians, and  $\alpha$  is the angle between the horizontal plane and spill hole border measured from the interior of the parachute in radians. The width of a panel is a function of the angle  $\gamma$ , which is defined to be between  $-\theta$  and  $\pi - \alpha$  in radians and stands as follows:

$$l = \frac{2\pi}{n} (R + r \cos(\gamma)) \quad (10)$$

Where  $l$  is the width,  $n$  is the number of panels on the parachute,  $R$  is the radius of revolution of the torus itself,  $r$  is the radius of the revolving circle and  $\gamma$  is some angle between  $-\theta$  and  $\pi - \alpha$  in radians.

It was chosen that the drogue parachute would be made out of 8 panels and the main parachute, 18 panels. We also considered the case where  $R = r$ . The suspension lines have a length  $S$  of 115% of the diameter of the parachute, thus  $1.15 \times 4R$ . The spill hole has a radius  $p$  of 15% the radius of the parachute, thus  $p = 0.15 \times 2R$ . When the parachute is fully inflated, suspension lines are supposed to be tangent to the parachute border, thus

$$\theta = \arctan\left(\frac{P}{H}\right) \approx \arcsin\left(\frac{R+r}{S}\right) = 0.449797 \text{ rad} \quad (11)$$

Following the same reasoning,

$$\alpha = \arctan\left(\frac{p}{h}\right) \approx \arccos\left(\frac{R-p}{r}\right) = 0.795399 \text{ rad} \quad (12)$$

By knowing these angles and the number of panels per parachute, a sewing pattern can be made as in the image below.



**Figure 38. Parachute panel patron**

The fabric used is an ultra-low-porosity nylon fabric used in reserves and main canopies. The panels and the suspension lines are then sewed with a Singer sewing machine and a nylon thread.



**Figure 39. Nylon fabric and sewing**

Once the fabrication was completed, several tests were conducted to ensure the resistance of the sewing. First, 45 pounds were suspended to simply make sure the parachute could hold a similar static weight as the rocket, see the images below.

Once we convinced ourselves of the efficiency of the parachutes, we moved outside simply to look at the parachutes fully opened to compare with the previous iterations and the geometry deficiencies we noted. The following images show the drogue and main parachutes fabricated.



**Figure 41. Sewing resistance test for the drogue**

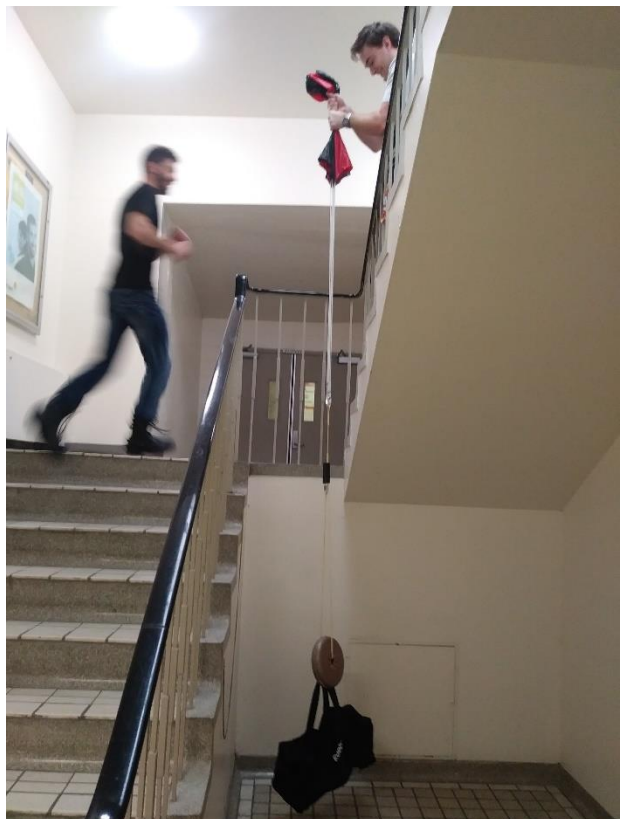


**Figure 40. Weight drop test**



**Figure 42. Sewing resistance test for the main**

Since the parachutes have successfully passed the static weight tests and the qualitative test outside, we are assured that they will safely recover the rocket at the competition.

#### 4. Deployment control

The deployment of the drogue and main parachutes can be triggered by two independent altimeters. The first is a commercial *StratoLogger* from *PerfectFlite*. This altimeter will be configured to deploy the drogue at apogee and the main at XX ft. This commercial altimeter is used as a backup for the second one. The second is a home-made altimeter and deployment system. It is powered by a 9V battery, uses a BMP180 to measure altitude, and a SD card to log the flight data. The data from the BMP180 is filtered using an elliptical low pass filter, generated by Matlab Ellip() function. The filter's parameters are:

- $N = 3$ , the order of the filter
- $W_p = 0.1$ , the cutoff frequency
- $R_p = 0.05$ , the peak-to-peak ripple
- $R_s = 40$ , the stopband attenuation

The filter's difference equation is as follows:

$$A_0 * y[n] + A_1 * y[n - 1] + A_2 * y[n - 2] + A_3 * y[n - 3] = B_0 * x[n] + B_1 * x[n - 1] + B_2 * x[n - 2] + B_3 * x[n - 3] \quad (13)$$

From the filtered altitude, the system computes the current speed using the average altitude increments from the last 4 filtered altitude data. The system detects the apogee by measuring the time since the filtered altitude last incremented. If more than 0.4 seconds have passed, the apogee is considered reached and the drogue is deployed. The main parachute is deployed simply when the filtered altitude reaches 460 meter, or 1509.19 ft, after the drogue has been deployed.

#### D. Payload Subsystems

For our 2018 payload, we decided to upgrade last year fiber optic gyroscope (FOG). A FOG is a Sagnac interferometer which is composed of the element shown in figure XY.

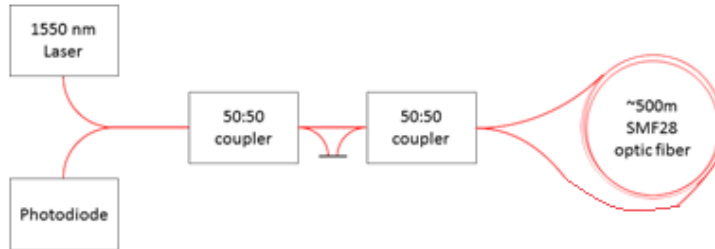


**Figure 43. FOG schematic**

#### FOG functioning

The FOG laser source is a 1550 nm HP™ LSC26 solid-state laser diode with a power of 5.3 mW. The same laser source is used for the 3 axes of the FOG. We divide the source a first time in 2 with a 72:25 coupler to make sure we have the greatest intensities in the 2 axes that interest us the most. The strongest branch is divided into 2 signals with a 50:50 coupler. Three branches are thus obtained: one of 25% and two others of 37.5%. The two most powerful axes are the ones for the yaw and the pitch of the rocket. For an optimal result of the Sagnac effect, it is necessary to ensure an equal optical path in both directions of passage of the optical circuit. To do this, two 50: 50 couplers from Thorlabs™ are used per axis. The part responsible for the Sagnac effect is a spherical three-axis coil. The coil was designed, and 3D printed at the University. Each axis of the coil comprises ~ 500 m of SMF-28 optical fiber with a core index of 1.467. The phase shift caused by the rotation of the interferometer is described by the following equation [4] : With this equation, it is possible to calculate the intensity of the laser seen at the photodiode. To do so, we calculated the electric field after the interference of the two beam counter propagating in the coil.

$$\phi_s = \frac{2\pi LD}{\lambda c} \Omega \quad (14)$$

The final equation can be seen below, where  $\Delta\phi$  is the sum of both the phase shift previously discussed:

$$I_d(t) = \frac{I_0}{2} [1 + \cos(\Delta\phi)] \quad (15)$$

#### E. Avionics Subsystems

The following section describes the four avionics subsystems. First, we'll look at how data is acquired on-board. Then we will describe how it is transmitted to the ground station, and how this ground station is designed.

### 1. On-board data acquisition

This year's data acquisition system is a simplified and more efficient version of 2017's version. This new version improves on the previous by using a better microcontroller to replace the AtMega328p from last year: the STM32F407. Using this chip has a lot of advantages: more memory, more processing power, better interrupt support, debugging support and much more.

The system has two sensors: a SparkFun Venus GPS and an Adafruit 9-DOF IMU breakout. The GPS is used to obtain the rocket's position at all times and the 9-DOF is used for 9 axes of data: 3 axes of accelerometer data, 3 axes gyroscopic, and 3 axes magnetic (compass).

### 2. Data transmission

The data transmission is designed on a three layers stack: the transport layer, the link layer and the physical layer.

The transport layer is fairly simple, the on-board microcontroller simply stores all the data as 32 bits floating point numbers in a data structure and writes one byte at a time over the link layer. The data is then received into the same structure on the other side of the link (i.e. the ground station).

The link layer protocol is the UART protocol, at a baud rate of 9600 bps and without the parity bit. The UART protocol simplifies communications, as it is an asynchronous protocol, which means the data can be transmitted on a single channel. To transmit UART over a wireless link, two RFD900 modulate the signal to the 900 MHz band.

The physical layer innovates on previous year by using homemade antennas. The first antenna, which is the on-board antenna, is a patch antenna which will be stick to the inside of the rocket. The second antenna is a directional Yagi antenna, which will be used by the ground station. This directional antenna will have to be aimed in the general direction of the rocket to receive the signal properly. The Figure 44 below shows the directivity of the Yagi antenna:

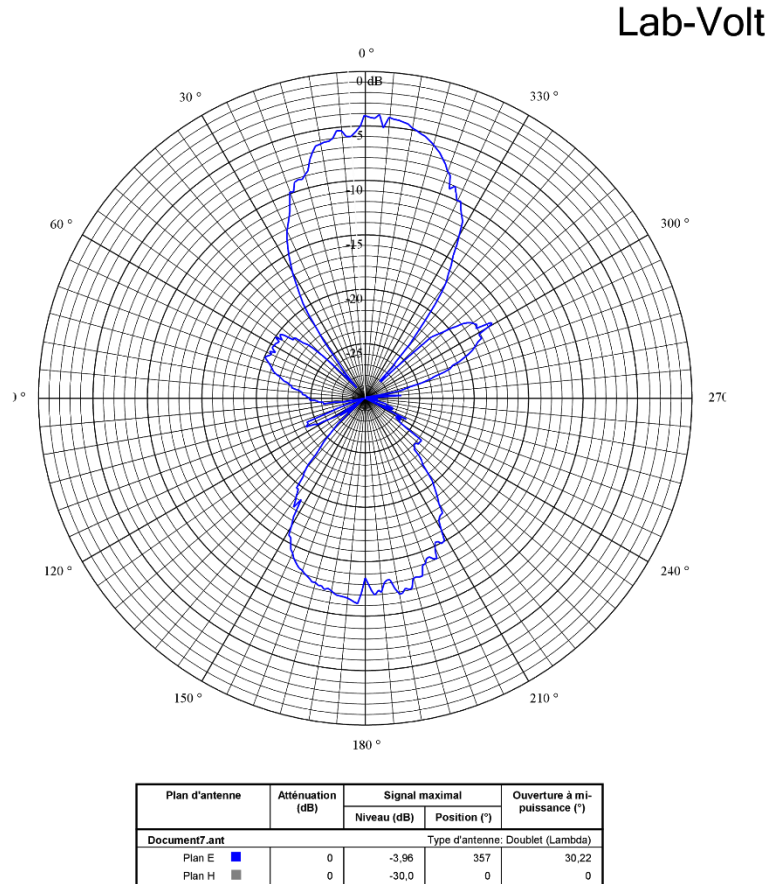


**Figure 44. Yagi antenna directivity**

### *3. Ground station*

Another great innovation for this year is the merge of the base station software with the mobile ground station from the previous years. This version has many new features:

- Improved casing
- 6.5-inch touchscreen
- Homemade keyboard
- OpenRocket software integration
- 3D real-time animation of the rocket
- Playback feature of the flight
- Rocket finder

To remain mobile and power efficient, the computer used is a Raspberry Pi 3B. The operating system used is the most recent version of Raspbian. Also, to locate the rocket, a SparkFun Venus GPS is used to compute position of the rocket in relation to the ground station. Since the Raspberry Pi 3B only has one UART bus (used for the data reception), a kernel module has been created to implement a UART bus on some unused GPIOs

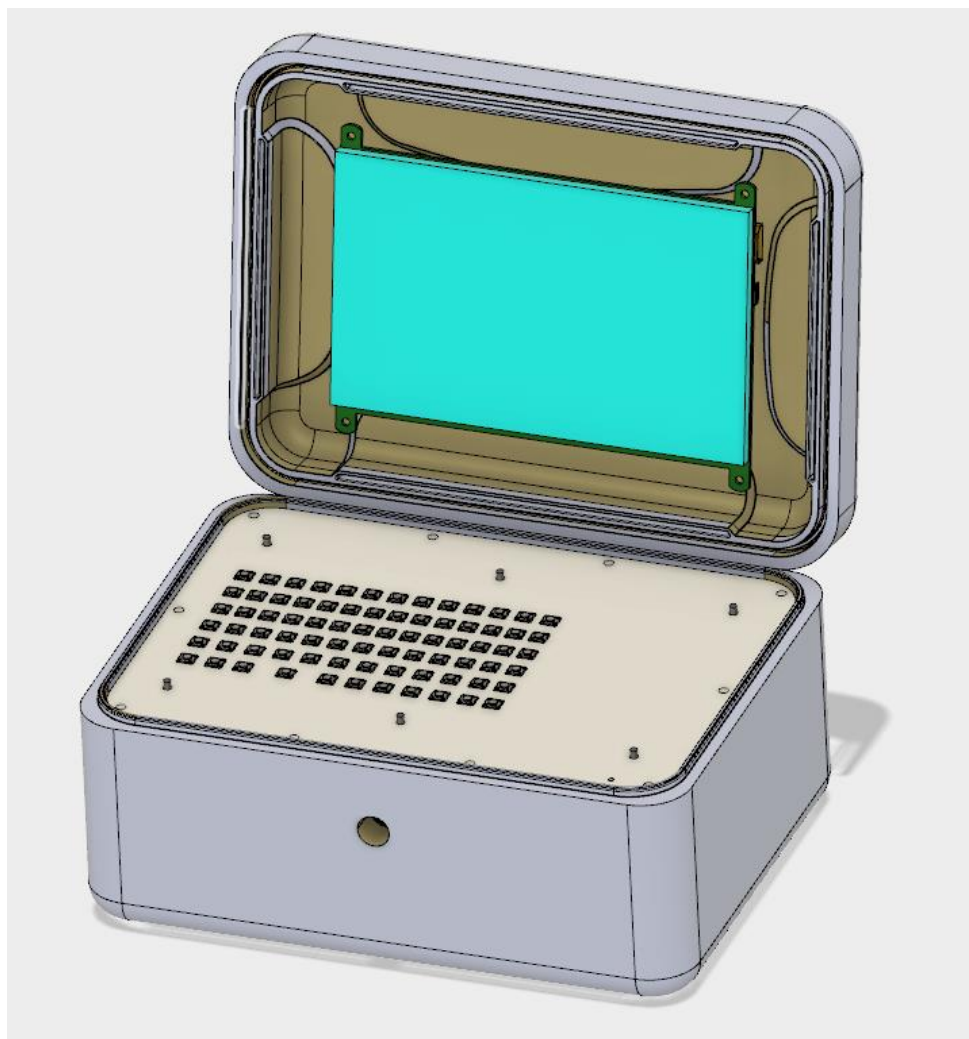


**Figure 45. Cad model of the ground station**

### III. Mission Concept of Operations Overview

The flight of the rocket is divided in 8 phases. Beginning with the preparation phase, where we bring the rocket to the launch pad, we will follow with the pre-launch phase, in which we are turning on the electronics and putting the electric match in the motor. We will then move on to the lift-off and the burn out, phases in which the rocket will begin and continue its motion. After that, the rocket will continue its ascent during the post-burn / pre-deployment phase. The transition of the next phase will occur when the the rocket will reach its apogee, at this moment, the drogue parachute will deploy. Then, at a predefine altitude, the main parachute will deploy, and the rocket will continue its descent until it lands. All the phases mentioned above are resumed in the table 1.

Table 1: Mission phases

Phase	Propulsion	Avionic	Payload	Recovery	Event for transition
<b>Preparation</b>	In safe position	Power is shutdown	Power is shutdown	In safe position	Turn on the power and arm the propulsion sub-systems
<b>Prelaunch</b>	In armed position	Powered on and acquiring data	Powered on and acquiring data	In armed position for both parachutes	Motor starting to burn
<b>Lift-off</b>	Burning	Powered on and acquiring data	Powered on and acquiring data	In armed position for both parachutes	Vehicle first motion
<b>Burnout</b>	Burning	Powered on and acquiring data	Powered on and acquiring data	In armed position for both parachutes	End of motor burnout
<b>Post-burn / Pre-deployment</b>	Non-energetic	Powered on and acquiring data	Powered on and acquiring data	In armed position for both parachutes	Ejection of the drogue parachute
<b>Descent under drogue</b>	Non-energetic	Powered on and acquiring data	Powered on and acquiring data	In armed position for the main parachute	Ejection of the main parachute
<b>Descent under main</b>	Non-energetic	Powered on and acquiring data	Powered on and acquiring data	Non-energetic	Touchdown
<b>Landing</b>	Non-energetic	Powered on and acquiring data	Powered on and acquiring data	Non-energetic	-

#### **IV. Conclusions and lessons learned**

During our 2017-2018 rocket project, new and older GAUL's members learned a lot about high power rocketry. We also worked of new approach of mixing the students off the different parts of the project to have more complete sub-systems. By example, our new avionic bay needed the work of students in mechanical engineering for the case and of students in electrical engineering for the electronic part. The same approach was also used for the payload and that helped us a lot. Instead of having separate teams, people were put in one big team from the start and this led to a better rocket.

As the project had new leaders, we learned the hard way about the need to have more time for most of the deadlines. Indeed, some of the date on our schedules were not respected and this is a thing to focus for the next season.

For the next season, we will continue to focus on implementing some formation on the techniques we are using, we will define new positions in the team to be sure we get everything on time. We are also proud to have designed an avionics bay that we will be able to reuse next year.

## Appendix

### A. System Weights, Measures, and Performance Data

Table 2: Overall rocket parameters

	Measurement	Additional Comments (Optional)
Airframe Length (inches):	131.5	
Airframe Diameter (inches):	6.2	
Fin-span (inches):	17.2	
Vehicle weight (pounds):	53.41	
Propellant weight (pounds):	9.79	
Payload weight (pounds):	8.8	
Liftoff weight (pounds):	72	
Number of stages:	1	
Strap-on Booster Cluster:	No	
Propulsion Type:	Solid	
Propulsion Manufacturer:	Commercial	
Kinetic Energy Dart:	No	

Table 3: Predicted flight data

	Measurement	Additional Comments (Optional)
Launch Rail:	Other	Rocketry Photography ramp (Doug Gerrard)
Rail Length (feet):	16	
Liftoff Thrust-Weight Ratio:	12.44	
Launch Rail Departure Velocity (feet/second):	100.7	
Minimum Static Margin During Boost:	2.35	*Between rail departure and burnout
Maximum Acceleration (G):	11.52	
Maximum Velocity (feet/second):	928.47	
Target Apogee (feet AGL):	10k	
Predicted Apogee Altitude (feet AGL):	10039	

## B. Project Test Reports

### Recovery System Testing

As explained in the recovery sub-section, The deployment of the drogue and main parachutes can be triggered by two independent altimeters. The first is a commercial *StratoLogger* from *PerfectFlite*. This altimeter will be configured to deploy the drogue at apogee and the main at 1505.19 ft. This commercial altimeter is used as a backup for the second one. The second is a home-made altimeter and deployment system. It is powered by a 9V battery, uses a BMP180 to measure altitude, and a SD card to log the flight data. The data from the BMP180 is filtered using an elliptical low pass filter, generated by Matlab Ellip() function. The filter's parameters are:

- $N = 3$ , the order of the filter
- $W_p = 0.1$ , the cutoff frequency
- $R_p = 0.05$ , the peak-to-peak ripple
- $R_s = 40$ , the stopband attenuation

The filter's difference equation is as follows:

$$A0*y[n]+A1*y[n-1]+A2*y[n-2]+A3*y[n-3]=B0*x[n]+B1*x[n-1]+B2*x[n-2]+B3*x[n-3]$$

From the filtered altitude, the system computes the current speed using the average altitude increments from the last 4 filtered altitude data. The system detects the apogee by measuring the time since the filtered altitude last incremented. If more than 0.4 seconds have passed, the apogee is considered reached and the drogue is deployed. The main parachute is deployed simply when the filtered altitude reaches 460 meter, or 1509.19 ft, after the drogue has been deployed.

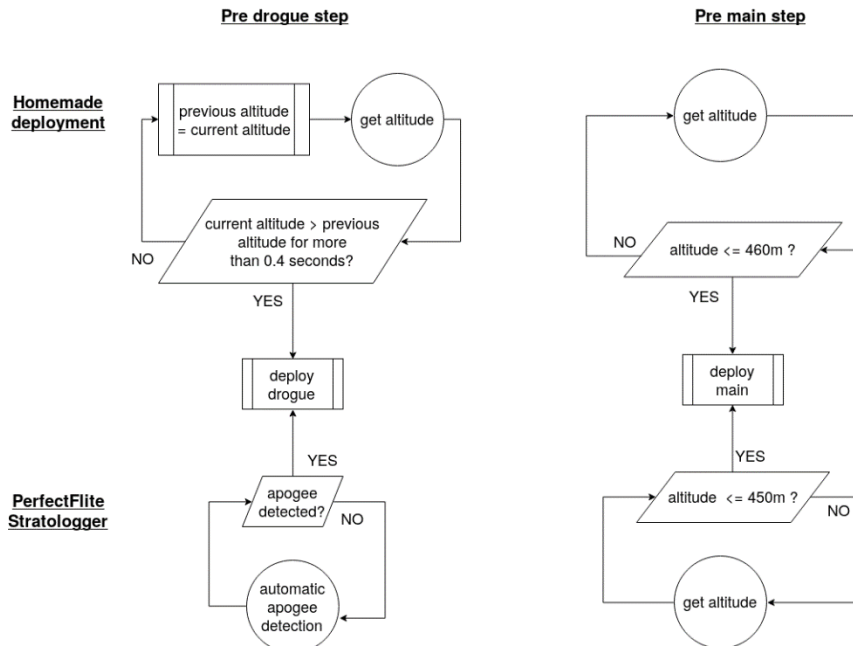


**Figure 46. Deployment schematic**

Since our rocket's fuselage was not yet assembled for the handover of the report, we performed our recovery test with our previous rocket Menhir. The test was made using the MK3 CO<sub>2</sub> recovery system with a 16g CO<sub>2</sub> cartridge and three 4-40 shear pins. The parachute compartment is 6in diameter by 45cm long. We put inside the main parachute wrapped in nomex. After everything was safe and ready to go we used a 9v battery to light up the match and the test was a success. The cold empty CO<sub>2</sub> cartridge was removed and disposed appropriately, and the CO<sub>2</sub> recovery system cleaned up from the black powder waste.

**SRAD Propulsion System Testing**

THIS PAGE INTENTIONALLY LEFT BLANK

**SRAD Pressure Vessel Testing**

THIS PAGE INTENTIONALLY LEFT BLANK

### C. Hazard Analysis

The table 4 present a list of the hazardous material with which we are working and the approach we do to mitigate the risks.

Table 4 : Hazard analysis table

Hazardous material	Mitigation approach
Epoxy	The epoxy containers are stored in a locked cabinet. When we are working with epoxy, we use <u>individual protection equipment</u> and we work in a local with an air curtain.
Black power	The black power is contained in small containers in a locked cabinet. We always bring small quantity for safety purpose. Also, we always put the match in the black power at the last moment and when we are sure the environment is safe.
CO <sub>2</sub> cartridge	We transport the CO <sub>2</sub> cartridge in a safe package without sharp object. We put the cartridge in the ejection system only when we are ready and when we are sure the environment is safe.
Motor	We receive the motor directly at the competition. We keep it in its package and in the shadow. We only assemble it before the launch and only the people that need to work on the motor and that are wearing <u>individual protection equipment</u> can be near it.

#### D. Risk Assessment

Team 42		Project: HIGH V		
<u>Hazard</u>	Possible Causes	Risk of Mishap and Rationale	Mitigation Approach	Risk of injury after mitigation
Explosion of solid propellant rocket motor during launch, with blast or flying debris causing injury.	Cracks in propellant grain	Low; Commercial-built motor from Cesaroni Technology. Pro 98 are deemed reliable and are very unlikely to explode.	Propellant grain is bought from MotoJoe Inc. and will be delivered to the team once on site.	Very Low
	Debonding of propellant from wall		Visual inspection of motor grain at delivery and before insertion into the casing.	
	Gap between propellant section and nozzle		Propellant grain will be secured in the casing using the appropriate methods while making sure the grip will not create fractures in the grain.	
	Chunk of propellant breaking off and plugging nozzle		Inspect motor case for damage during final assembly before launch.	
	Motor case unable to contain normal operating pressure		Only essential personnel in launch crew, motor casing has been checked by a technical advisor.	
	Motor end closures fail to hold		Launch crew 200 feet from rocket at launch, behind rudimentary blastshield (vehicle).	
	Rocket became unstable after launch		After simulations with Open Rocket, CG was moved to ensure that no construction errors would dramatically affect flight performance. Stability is around 2.35 calibers.	
Rocket deviates from nominal flight path, comes in contact with	Rocket fins were not strong enough to support deviation constraints	Medium; student-built airframe with limited testing and numerical simulations	Rocket fins base have been reinforced with carbon fiber. The gap between the fins and the outer shell have been sealed with putty and another layer of carbon fiber following the tip-to-tip method.	Low

personnel at high speed.				
Recovery system fails to deploy, rocket or payload comes in contact with personnel	Primary system malfunction	Medium; student-built avionics with limited testing	Deployment system has been doubled, in case of missfire or bad pressurisation there will be a second black powder detonation.	Medium-Low
	Electrical system malfunction	Medium; student-built avionics with limited testing	Avionics has a backup system with independent power source	
Recovery system partially deploys, rocket or payload comes in contact with personnel	Primary parachute did not open properly	Low; Commercial-built parachute stored in recovery bay	Two e-matches are used to ensure deployment.	Low
Recovery system deploys during assembly or prelaunch, causing injury	Avionics systems program has a fault	Low; student-built avionics with altitude-based deployment	Only essential personnel (launch crew) to connect deployment system, protective equipment must be worn at all times when dealing with energetics.	Low
Main parachute deploys at or near apogee, rocket or payload drifts to highway(s)	Main parachute bay opens prematurely	Low; student-built mechanism with adequate testing	Deployment is planned at apogee to reduce stress	Low
			Only essential personnel (launch crew) to troubleshoot	Low

Rocket does not ignite when command is given (“hang fire”), but does ignite when team approaches to troubleshoot	Electrical match malfunction	Low; Commercial electrical matches with no misfire up to now		
Rocket falls from launch rail during prelaunch preparations, causing injury	Rail buttons break, letting the rocket fall	Low; Commercial components screwed onto rocket's hardpoints	Only essential personnel (launch crew) to install rocket on launch rail	Low

## **E. Assembly, Preflight, and Launch Checklists**

### **Assembly Checklist**

- Arrange the avionics systems and the payload in their respective CubeSat
- Integrate the avionics systems and the payload in the middle part of the rocket and fix the first bulkhead
- Pack the parachutes and insert them in their respective tubes.
- Prepare and integrate the deployment system
- Insert and fix the second bulkhead
- Attach the parachute to the second bulkhead
- Fix the tubes to the couplers
- Prepare and insert the motor (as seen on the instruction given by Cesaroni)

### **Preflight Checklist**

- Parachute well packed
- Engine well assembled
- Put the rocket on the launch rail and rise it
- Connect the power control connector and flip the following relay
  - Avionic 1 & 2
  - Camera
  - Payload
  - SRAD recovery
  - Stratologger

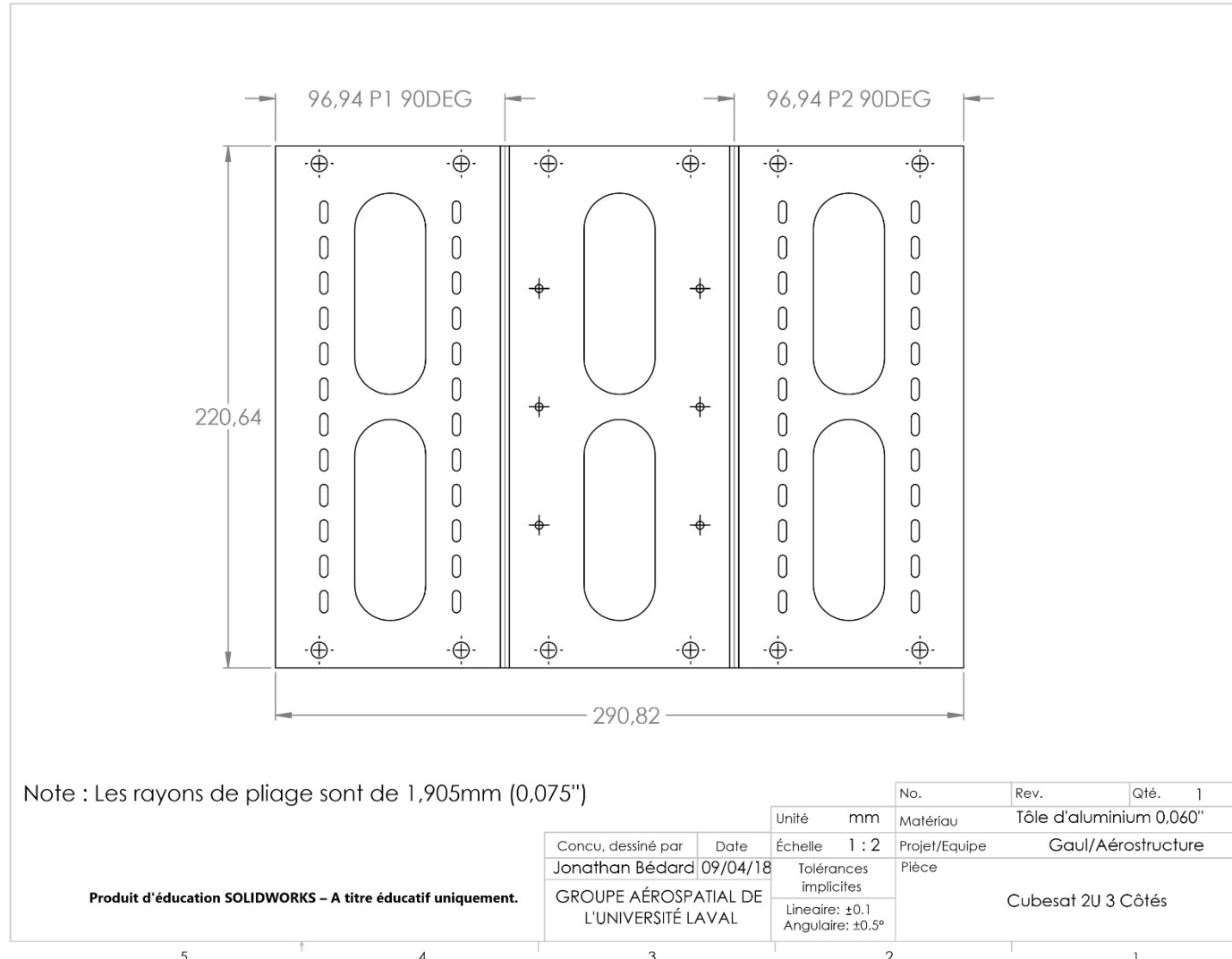
### **Launch Checklist**

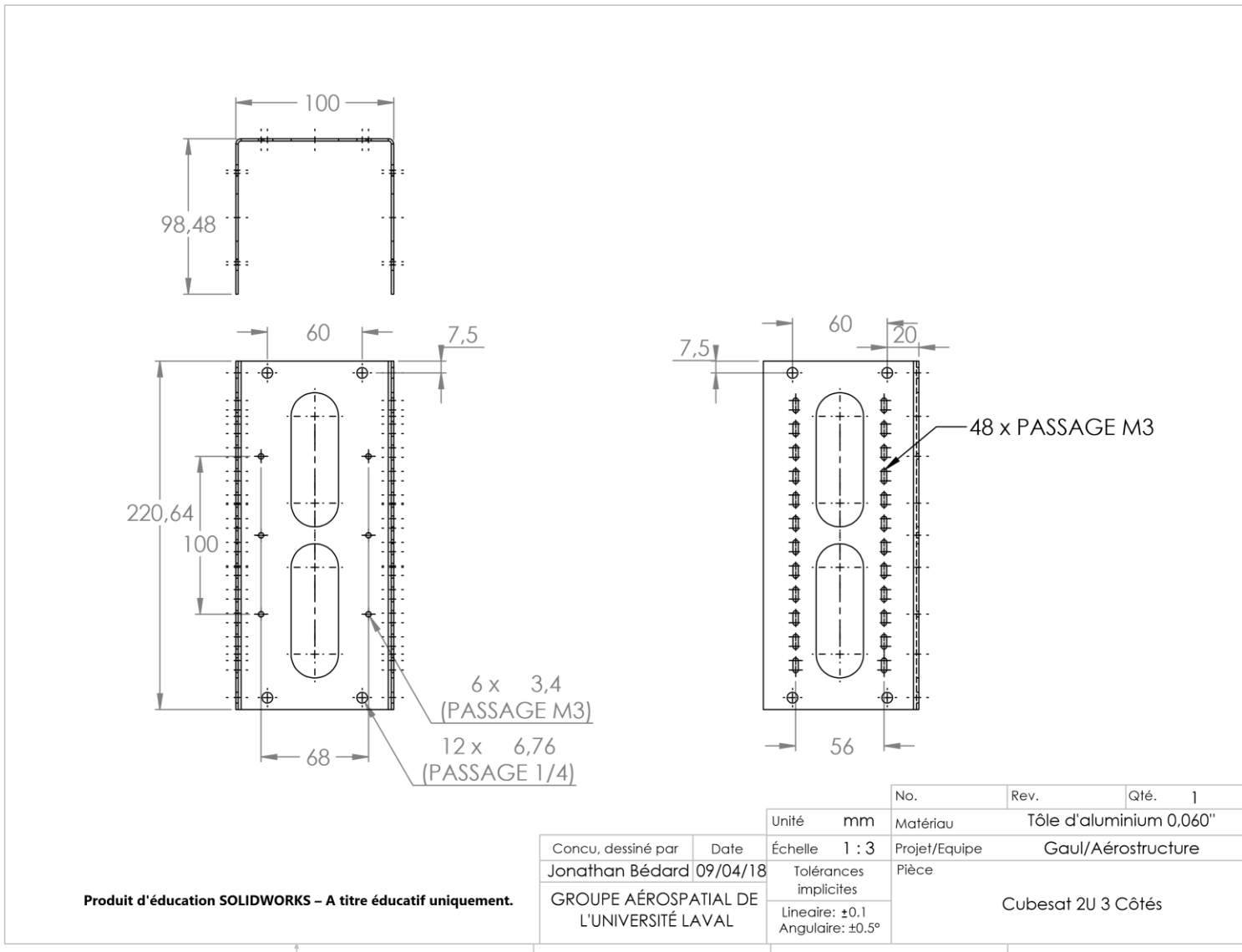
- Get sure the surrounding of the rocket is safe
- Put the electric match in the motor
- Go to a safe emplacement
- Make sure the environment (and the sky) is safe for a launch
- Fire the rocket (at the end of the countdown)

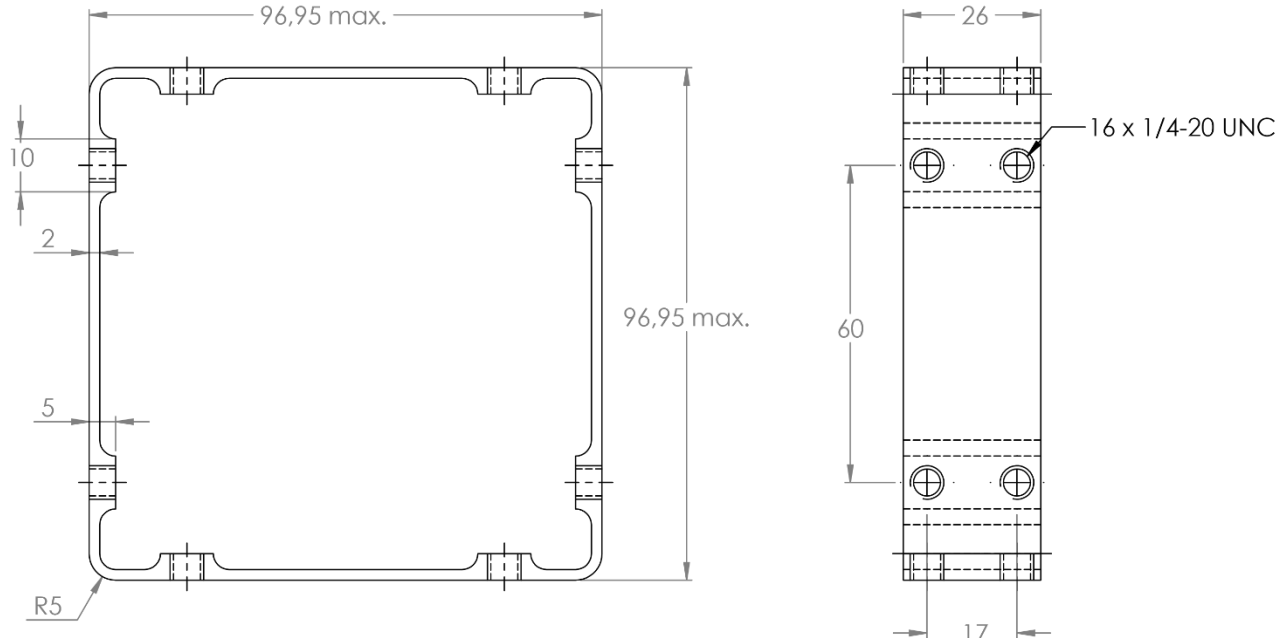
### **Abort Checklist**

- Wait the amount of time needed depending on the type of failure
- Make sure the remote to fire the motor is off
- Remove the electric match from the motor
- Turn off both of the altimeter
- Inspect the rocket

## F. Engineering Drawings





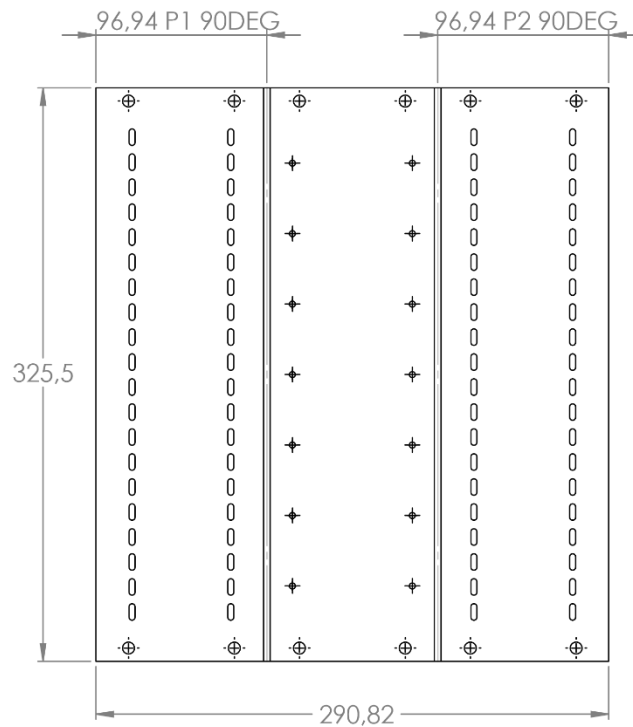


Note : Les congés sont R3.  
Les congés peuvent ne pas être respecté  
et être usinés avec un outil au choix.

**Produit d'éducation SOLIDWORKS – A titre éducatif uniquement.**

No.	Rev.	Qté.
		1
Unité	mm	Matériau
		Aluminium
Concu, dessiné par	Date	Échelle
Jonathan Bédard	16/04/18	1 : 1
GROUPE AÉROSPATIAL DE	Tolérances	Projet/Equipe
L'UNIVERSITÉ LAVAL	implicites	Gaul/Aérostructure
	Lineaire: ±0,1	Pièce
	Angulaire: ±0,5°	Liaison Cubesats

5      †      4      3      2      1

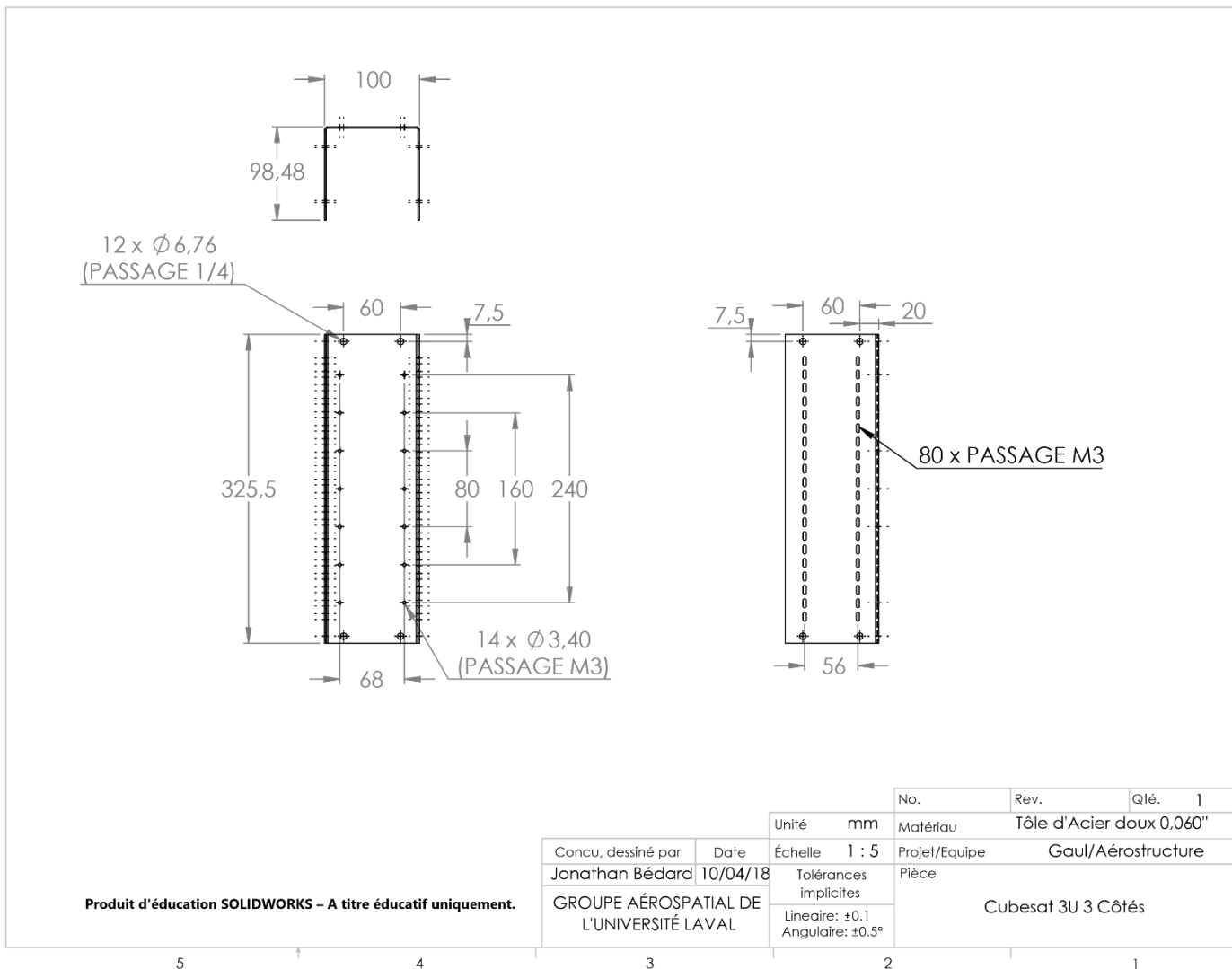


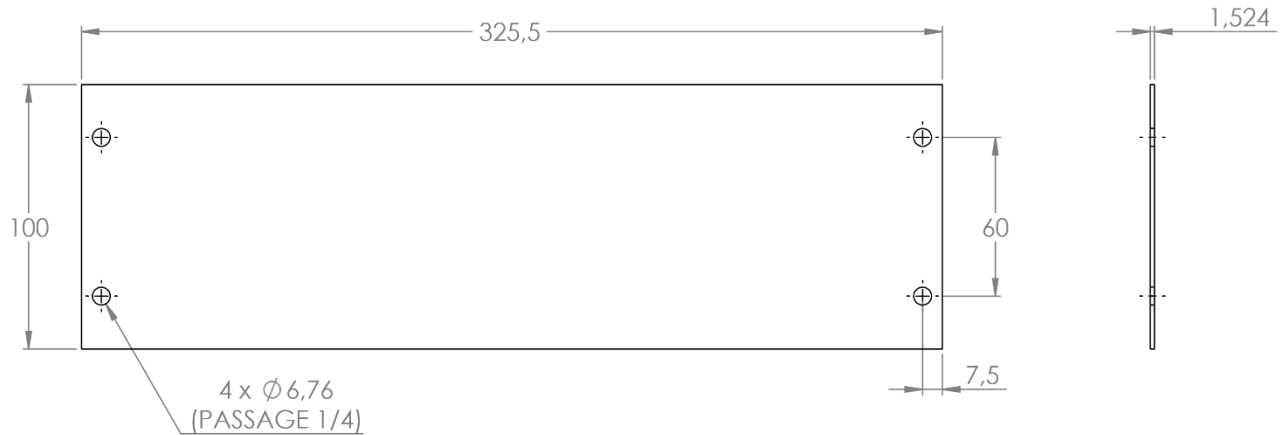
Note : Les rayons de pliage sont de 1,905mm (0,075")

**Produit d'éducation SOLIDWORKS – A titre éducatif uniquement.**

No.	Rev.	Qté.
Unité	mm	Matériau
Concu, dessiné par	Date	Tôle d'Acier doux 0,060"
Jonathan Bédard	10/04/18	Échelle 1 : 3 Projet/Equipe Gaul/Aérostructure
GROUPE AÉROSPATIAL DE L'UNIVERSITÉ LAVAL		Tolérances implicites Pièce
		Lineaire: ±0,1 Cubesat 3U 3 Côtés Déplié Angulaire: ±0,5°

5 † 4 3 2 1

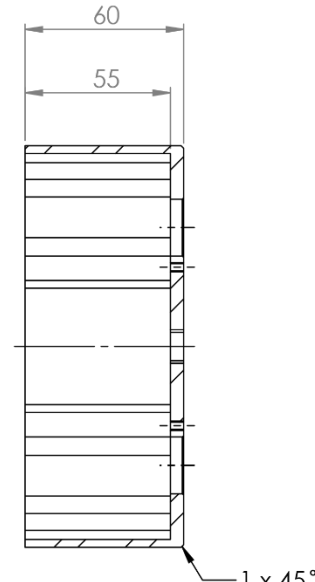
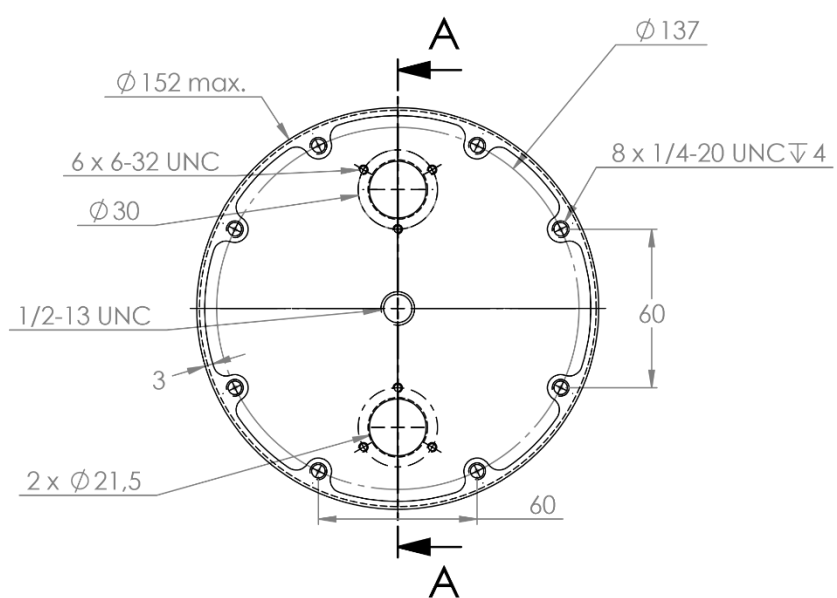




Produit d'éducation SOLIDWORKS – A titre éducatif uniquement.

Concu, dessiné par	Date	Unité	mm	No.	Rev.	Qté.
Jonathan Bédard	16/04/18	Échelle	1 : 2	Matériau	Tôle d'Acier doux 0,060"	1
		Tolérances implicites		Projet/Equipe	Gaul/Aérostructure	
		Lineaire: $\pm 0,5$	Angulaire: $\pm 0,5^\circ$	Pièce	Cubesat 3U Porte	

5                    4                    3                    2                    1



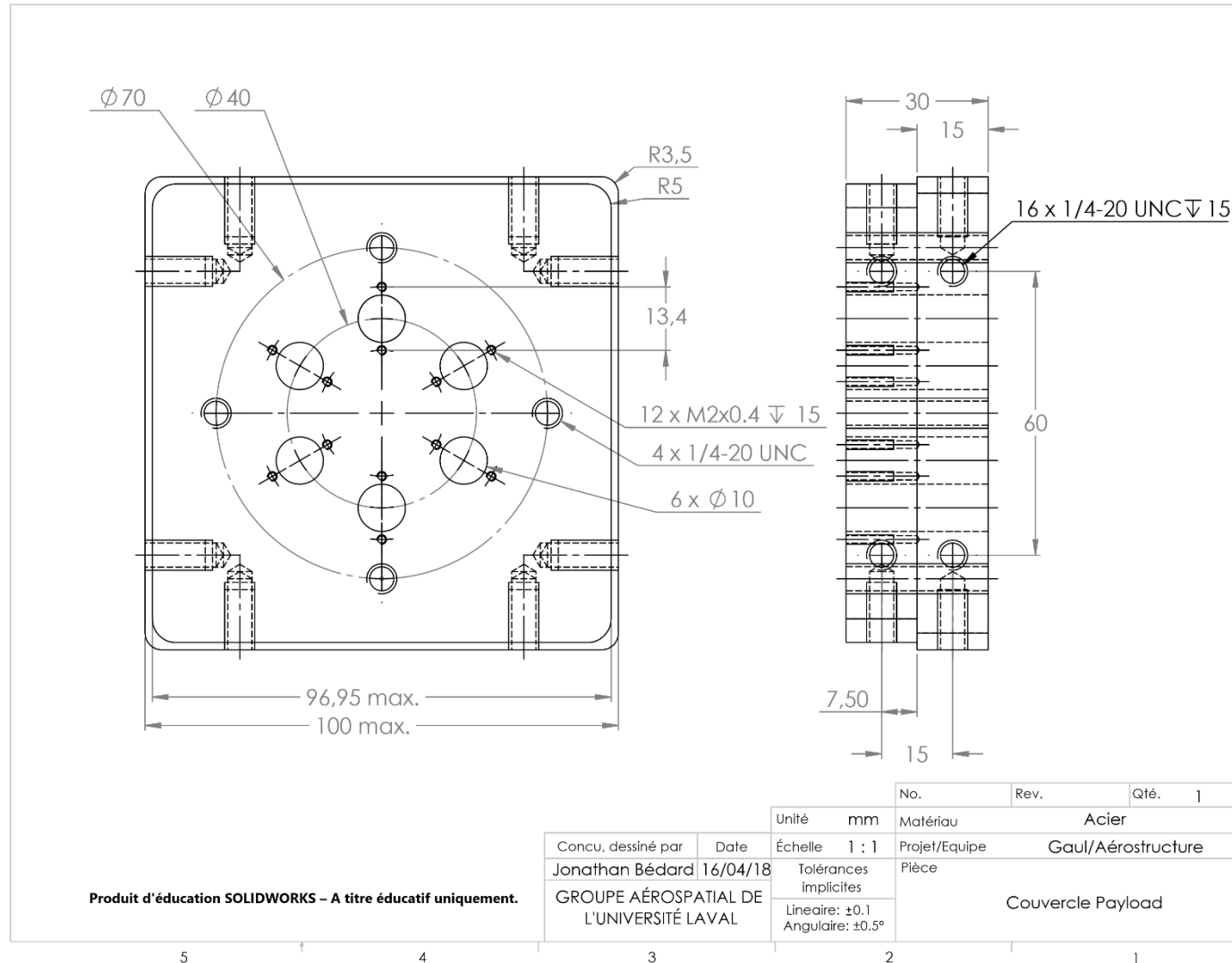
**COUPE A-A**

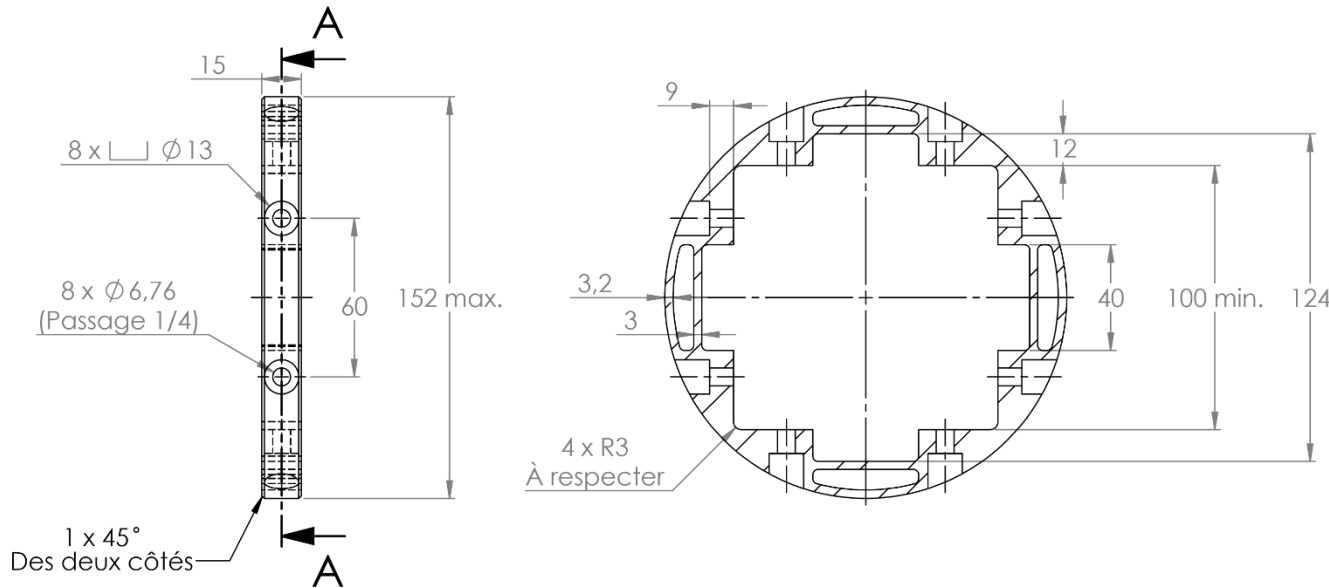
Note : Congés et arondis R5  
 Les congés peuvent ne pas être respecté  
 et être usinés avec un outil au choix.

**Produit d'éducation SOLIDWORKS – A titre éducatif uniquement.**

No.	Rev.	Qté.
		1
Unité	mm	Matériau
		Aluminium
Concu, dessiné par	Date	Échelle
Jonathan Bédard	16/04/18	1 : 2
GROUPE AÉROSPATIAL DE	Tolérances	Projet/Equipe
L'UNIVERSITÉ LAVAL	implicites	Gaul/Aérostructure
	Lineaire: ±0,1	Pièce
	Angulaire: ±0,5°	Bulkhead Avionique

5      †      4      3      2      1





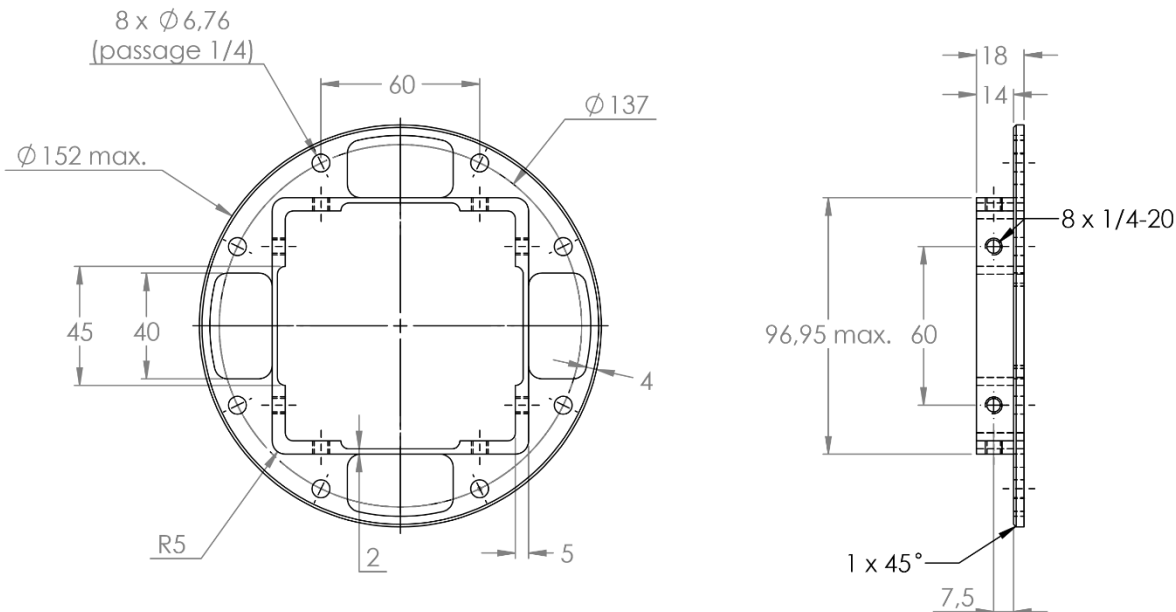
COUPE A-A

Note : Les autres congés sont R2.  
Ces congés peuvent ne pas être respecté  
et être usinés avec un outil au choix.

Produit d'éducation SOLIDWORKS – A titre éducatif uniquement.

	No.	Rev.	Qté.
Concu, dessiné par	Date	Unité	mm
Jonathan Bédard	16/04/18	Matériau	Aluminium
GROUPE AÉROSPATIAL DE		Échelle	1 : 2
L'UNIVERSITÉ LAVAL		Tolérances	Projet/Equipe
		implicites	Gaul/Aérostructure
		Lineaire: ±0,1	Pièce
		Angulaire: ±0,5°	Épaulement Payload

5 † 4 3 2 1

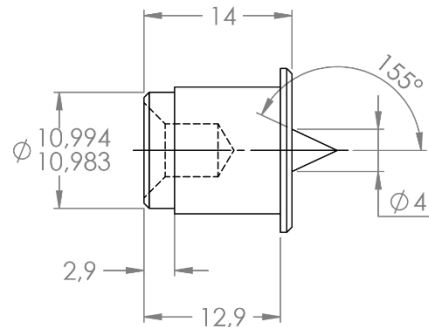
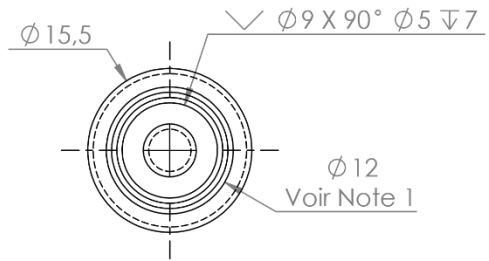


Note : Les autres congés sont R3.  
Les congés peuvent ne pas être respecté  
et être usinés avec un outil au choix.

Produit d'éducation SOLIDWORKS – A titre éducatif uniquement.

No.	Rev.	Qté.
Unité	mm	Matériau
Concu, dessiné par	Date	Échelle 1 : 2
Jonathan Bédard	16/04/18	Tolérances implicites
GROUPE AÉROSPATIAL DE L'UNIVERSITÉ LAVAL		Lineaire: $\pm 0.1$ Angulaire: $\pm 0.5^\circ$
		Projet/Equipe Gaul/Aérostructure
		Pièce Liaison Bulkhead-Cubesat Avionique
		1

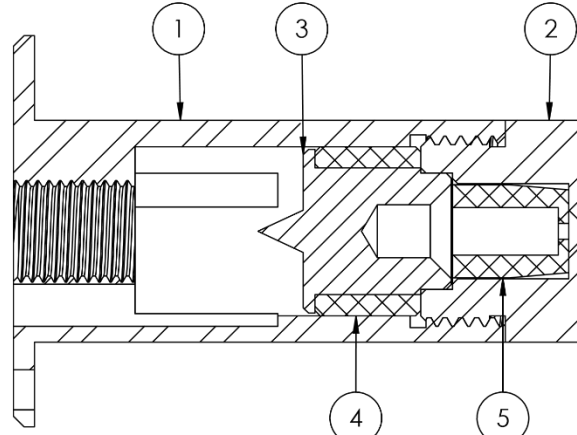
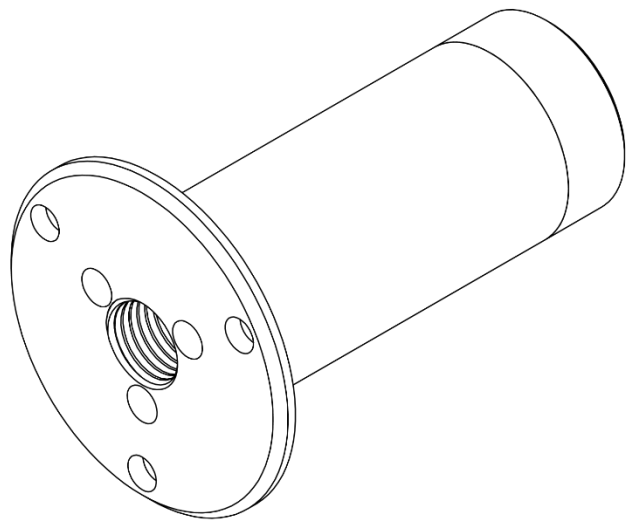
5 † 4 3 2 1



Note 1 : Le palier lisse devra être assemblé en serrage sur cette surface.

Produit d'éducation SOLIDWORKS – A titre éducatif uniquement.

		No.	3	Rev.	3	Qté.	4
Unité	mm	Matériau		Acier			
Concu, dessiné par		Échelle		Projet/Equipe			
Jonathan Bédard	31/03/18	2:1		GAUL/Aérostructure			
GROUPE AÉROSPATIAL DE L'UNIVERSITÉ LAVAL		Tolérances implicites		Pièce			
		Lineaire: ±0,5 Angulaire: ±0,5°		Percuteur MK3   Déploiement			



- 1 : Canon MK3  
2 : Base MK3  
3 : Percuteur MK3  
4 : Palier lisse  
5 : Tube Alumette Jetable(Non Demandé)

Produit d'éducation SOLIDWORKS – A titre éducatif uniquement.

Unité	mm	No.	Rev.	Qté.
Concu, dessiné par	Date	3	3	4
Jonathan Bédard	31/03/18	Échelle	2:1	Matériau
		Tolérances		Projet/Equipe
		implicites		GAUL/Aérostructure
		Lineaire: ±0.5		Pièce
		Angulaire: ±0.5°		Assemblage Déploiement CO2 MK3

5

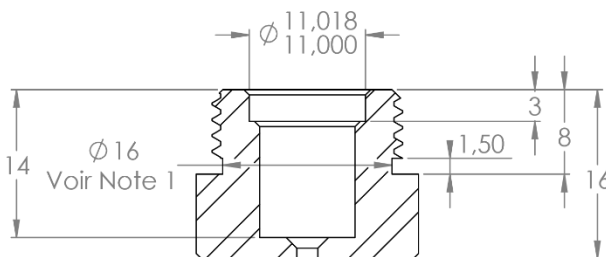
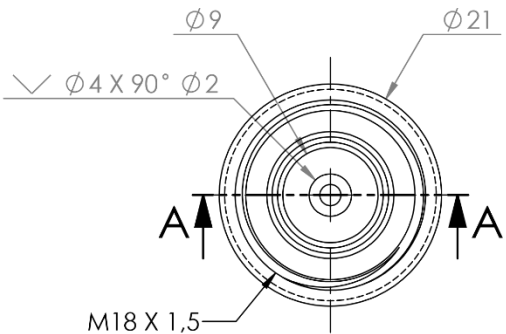
†

4

3

2

1



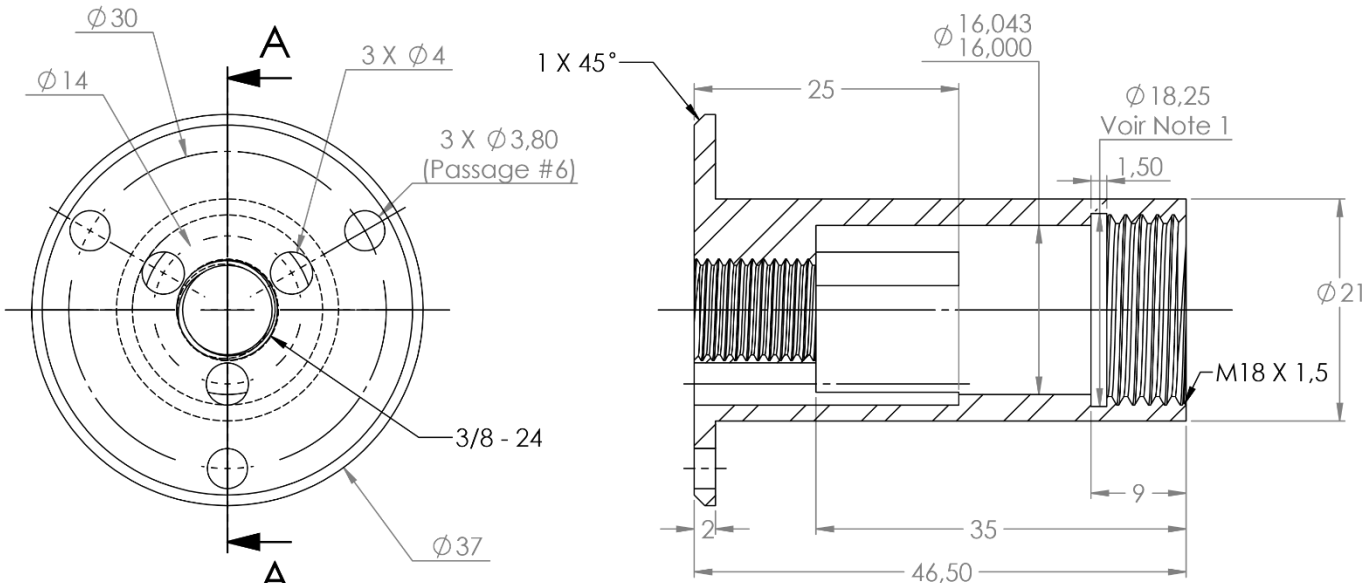
**COUPE A-A**

Note 1: Rainure de dégagement de filetage

**Produit d'éducation SOLIDWORKS – A titre éducatif uniquement.**

No.	2	Rev.	3	Qté.	4
Unité	mm	Matériau	Aluminium		
Concu, dessiné par	Date	Échelle	2:1	Projet/Equipe	GAUL/Aérostructure
Jonathan Bédard	31/03/18	Tolérances implicites		Pièce	
GROUPE AÉROSPATIAL DE L'UNIVERSITÉ LAVAL		Lineaire: ±0,5 Angulaire: ±0,5°		Base MK3   Déploiement	

5 † 4 3 2 1

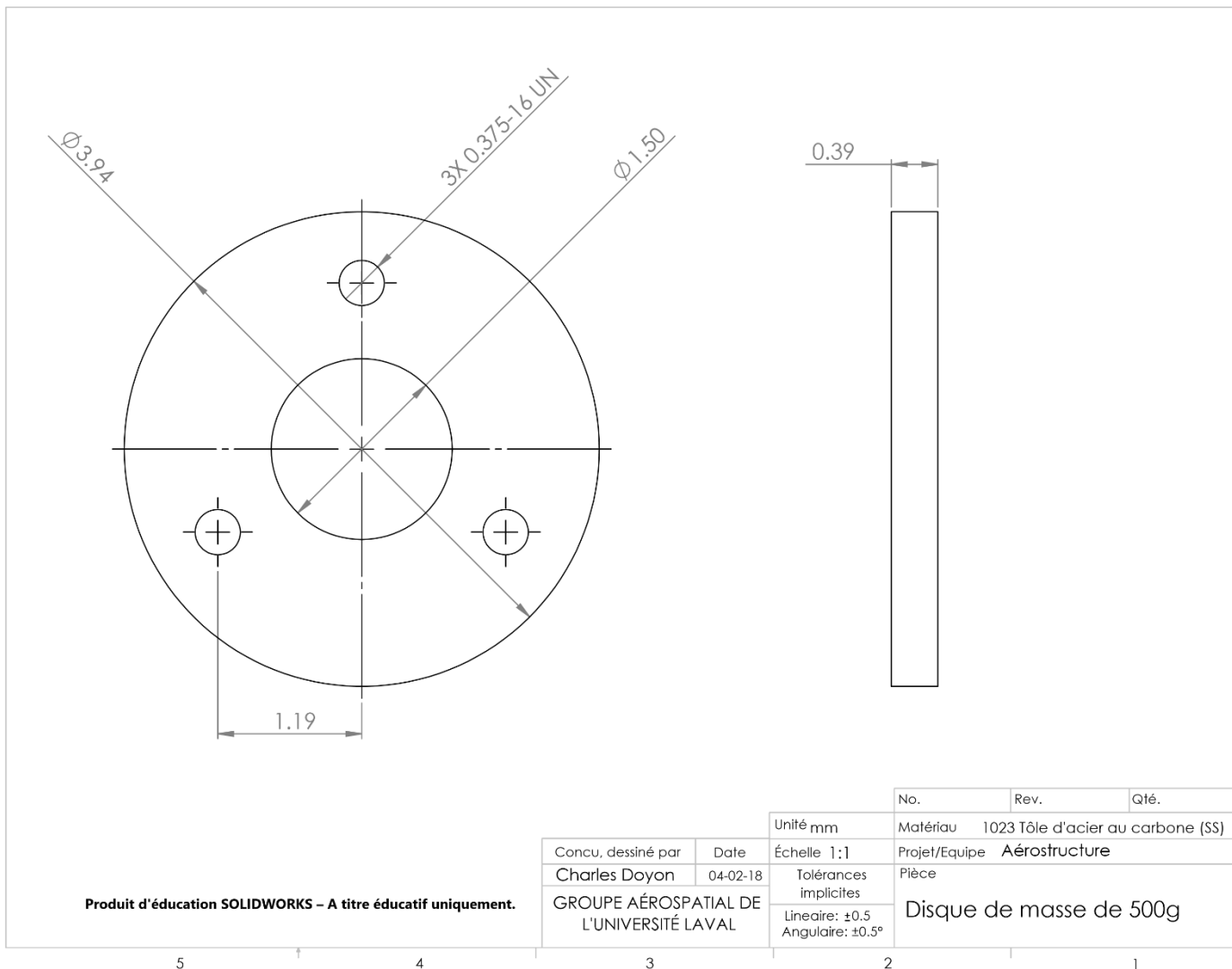


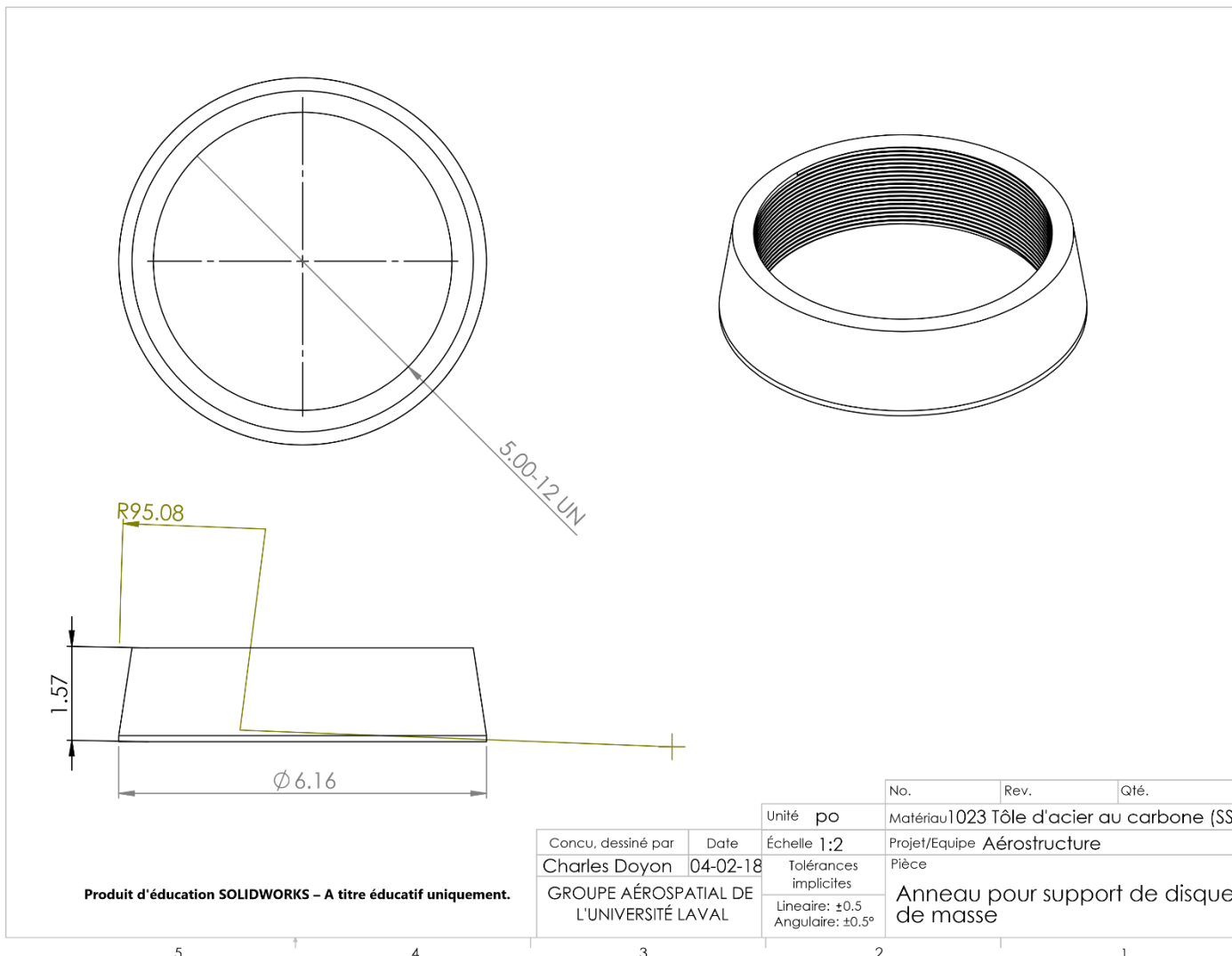
**COUPE A-A**

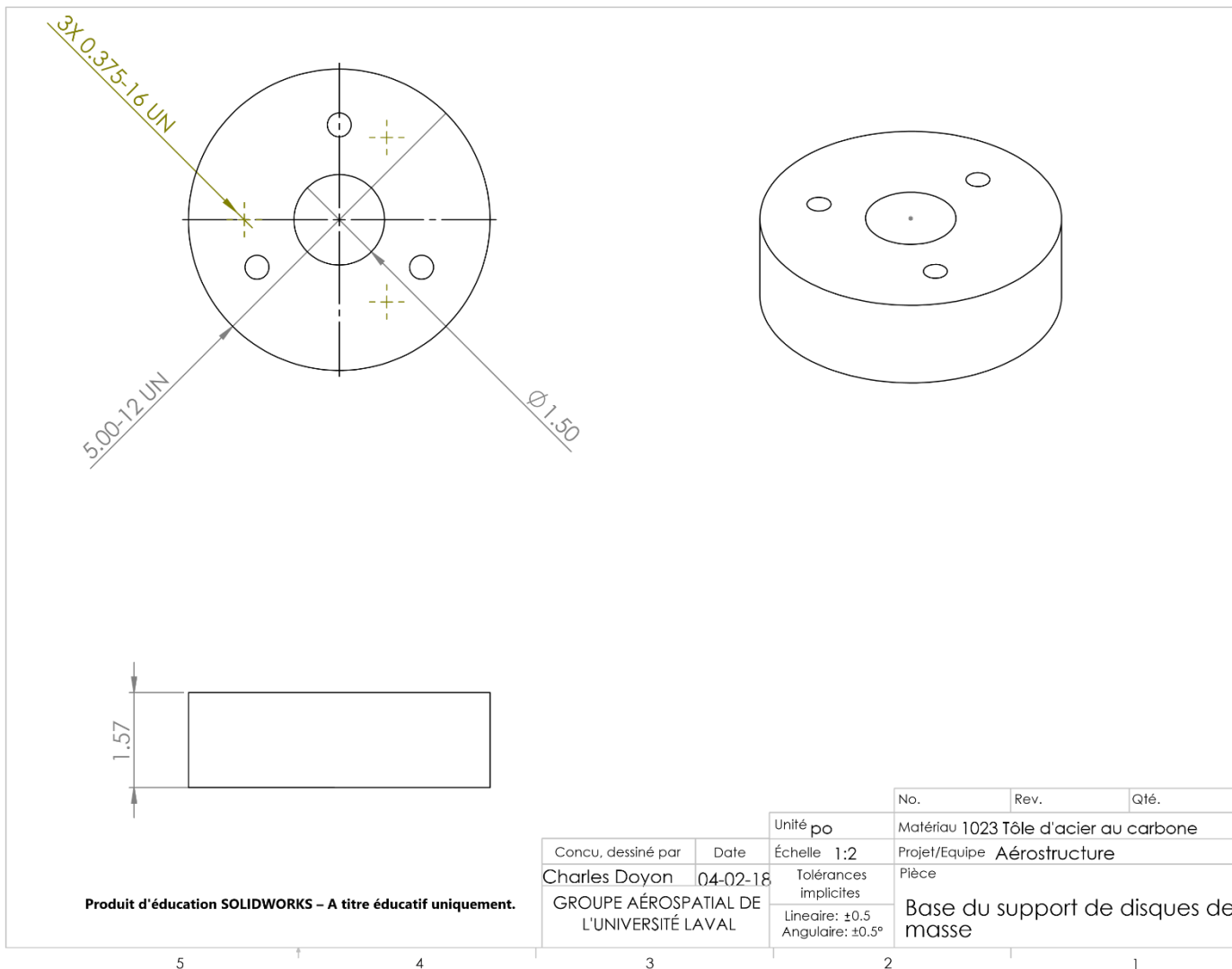
Note 1: Rainure de dégagement de filetage

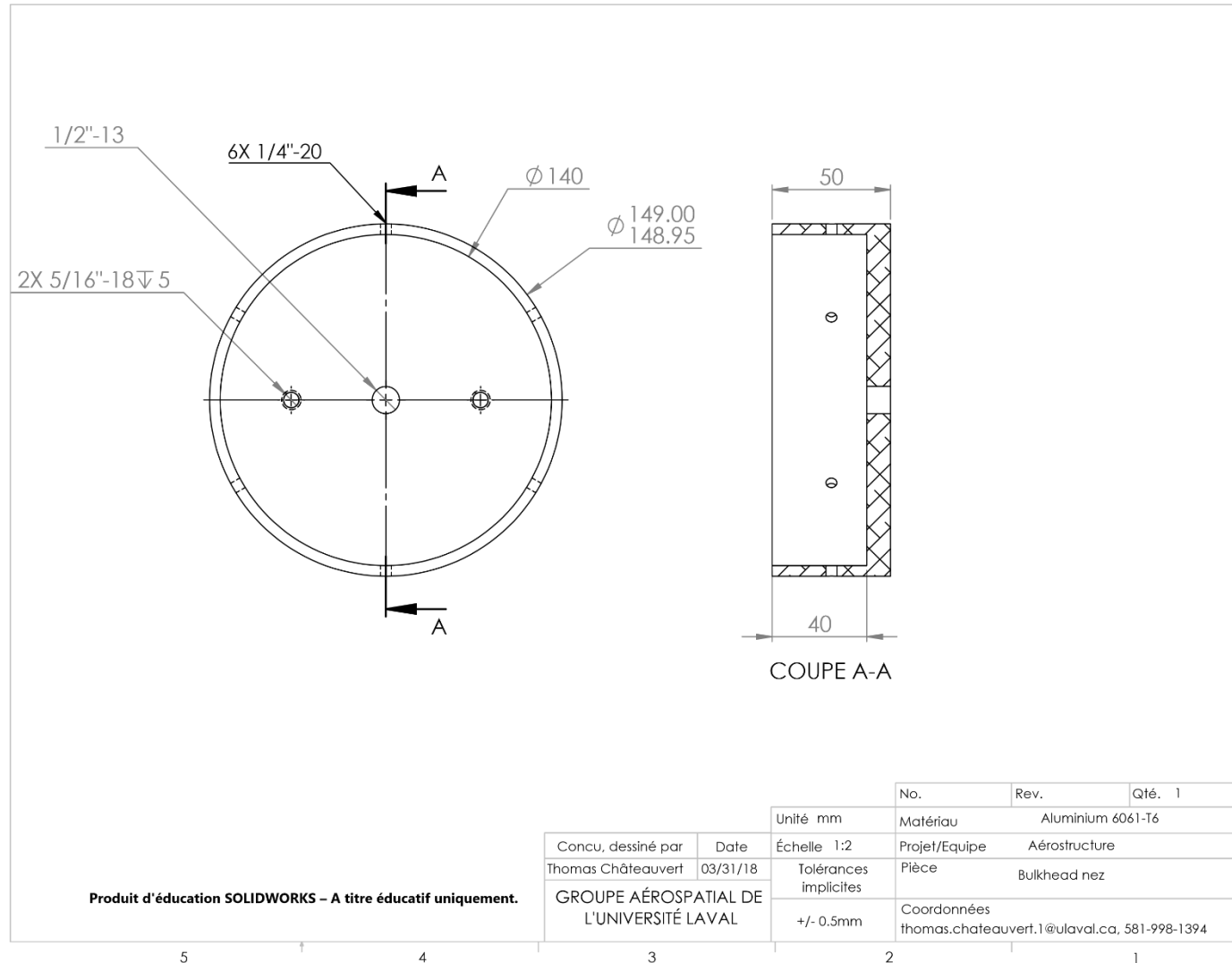
Produit d'éducation SOLIDWORKS – A titre éducatif uniquement.

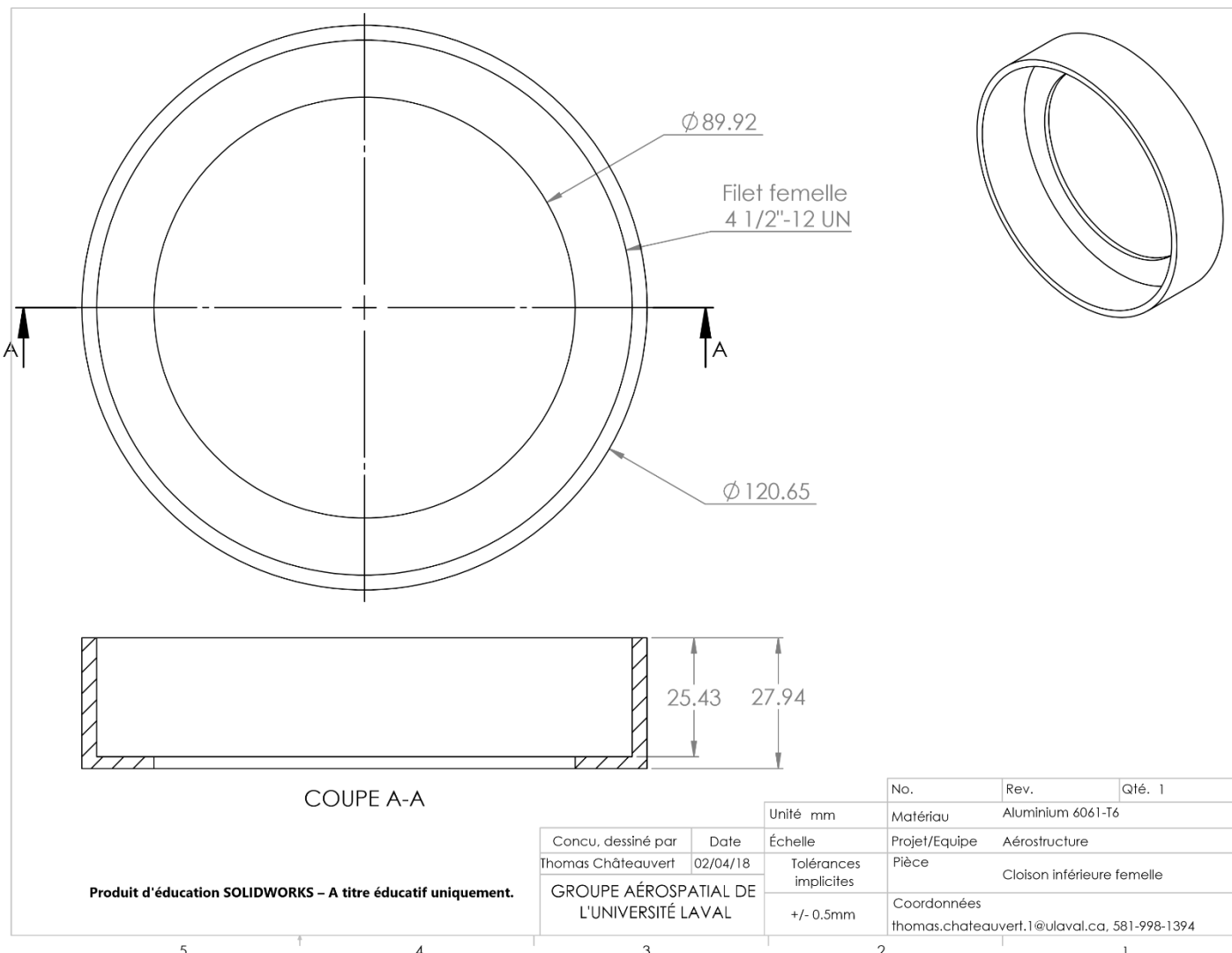
No.	1	Rev.	3	Qté.	4
Unité	mm	Matériau	Aluminium		
Concu, dessiné par	Date	Échelle	2:1	Projet/Equipe	GAUL/Aérostructure
Jonathan Bédard	31/03/18	Tolérances implicites		Pièce	
GROUPE AÉROSPATIAL DE L'UNIVERSITÉ LAVAL		Lineaire: ±0.5 Angulaire: ±0.5°		Canon MK3   Déploiement	

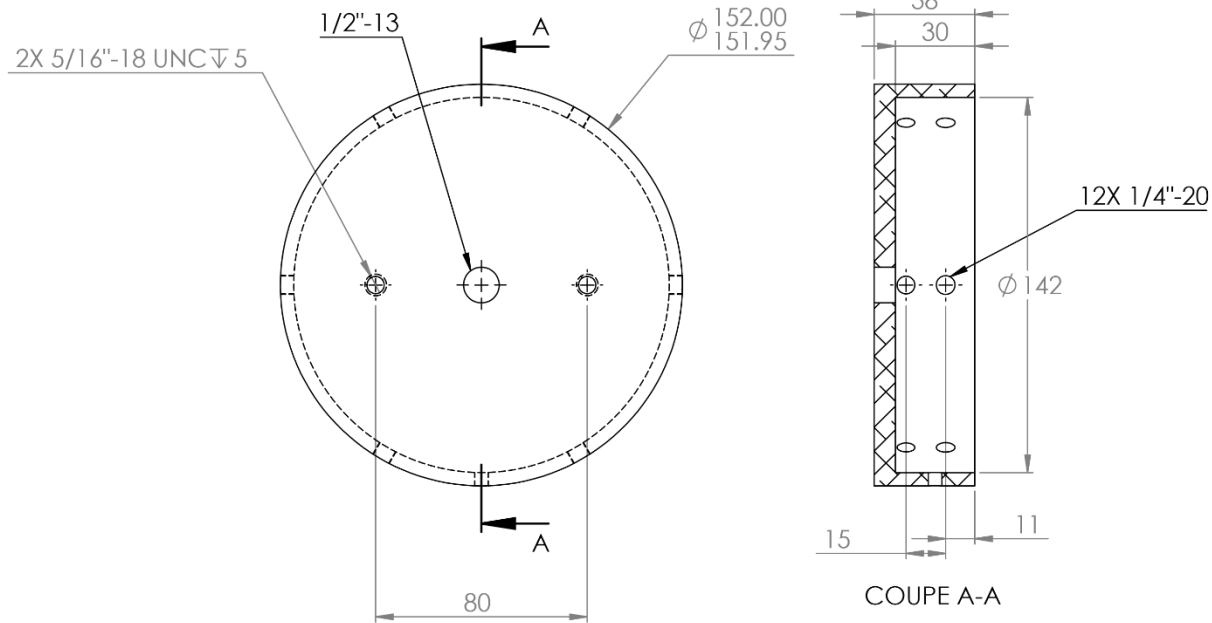












Produit d'éducation SOLIDWORKS – A titre éducatif uniquement.

Concu, dessiné par Thomas Châteauvert	Date 04/02/18
GROUPE AÉROSPATIAL DE L'UNIVERSITÉ LAVAL	
Unité mm	Matériau Aluminium 6061-T6
Échelle 1:2	Projet/Equipe Aérostructure

No.	Rev.	Qté. 1
Tolérances implicites	Pièce Cloison supérieure	
+/- 0.5mm	Coordonnées thomas.chateauvert.1@ulaval.ca, 581-998-1394	

5 † 4 3 2 1

